

DEVELOPMENT OF TETRAHYDROCURCUMIN-LOADED  
CHITOSAN-COATED-NANOSTRUCTURED LIPID  
CARRIERS FOR TOPICAL TREATMENT OF PSORIASIS



A Thesis Submitted in Partial Fulfillment of the Requirements  
for the Degree of Master of Science in Pharmaceutical Sciences and  
Technology

Common Course

FACULTY OF PHARMACEUTICAL SCIENCES

Chulalongkorn University

Academic Year 2021

Copyright of Chulalongkorn University

การพัฒนาตัวพลาสมาของลิพิดที่เคลือบด้วยไคโตซานที่บรรจุด้วยสารเตตระไฮโดรเคอร์คูมิน  
สำหรับการรักษาโรคสะเก็ดเงินเฉพาะที่



วิทยานิพนธ์นี้เป็นส่วนหนึ่งของการศึกษาตามหลักสูตรปริญญาวิทยาศาสตรมหาบัณฑิต  
สาขาวิชาเภสัชศาสตร์และเทคโนโลยี ไม่สังกัดภาควิชา/เทียบเท่า  
คณะเภสัชศาสตร์ จุฬาลงกรณ์มหาวิทยาลัย  
ปีการศึกษา 2564  
ลิขสิทธิ์ของจุฬาลงกรณ์มหาวิทยาลัย

Thesis Title                                   DEVELOPMENT OF TETRAHYDROCURCUMIN-  
LOADED CHITOSAN-COATED-  
NANOSTRUCTURED LIPID CARRIERS FOR  
TOPICAL TREATMENT OF PSORIASIS

By   Mr. Hoang Thien Truong

Field of Study                                Pharmaceutical Sciences and Technology

Thesis Advisor                               Associate Professor PORNCHAI ROJSITTHISAK,  
Ph.D.

Thesis Co Advisor                           Associate Professor Pranee Rojsitthisak, Ph.D.  
Professor OPA VAJRAGUPTA, Ph.D.

---

Accepted by the FACULTY OF PHARMACEUTICAL SCIENCES,  
Chulalongkorn University in Partial Fulfillment of the Requirement for the Master of  
Science

..... Dean of the FACULTY OF  
PHARMACEUTICAL SCIENCES  
(Professor PORNANONG ARAMWIT, Ph.D.)

THESIS COMMITTEE

..... Chairman  
(Assistant Professor JITTIMA CHATCHAWALSAISIN,  
Ph.D.)

..... Thesis Advisor  
(Associate Professor PORNCHAI ROJSITTHISAK,  
Ph.D.)

..... Thesis Co-Advisor  
(Associate Professor Pranee Rojsitthisak, Ph.D.)

..... Thesis Co-Advisor  
(Professor OPA VAJRAGUPTA, Ph.D.)

..... Examiner  
(Assistant Professor CHATCHAI CHAOTHAM, Ph.D.)

..... External Examiner  
(Professor ETSUO YONEMOCHI, Ph.D.)

ชวง เทียน ตรอง : การพัฒนาตัวพาขนาดนาโนของลิพิดที่เคลือบด้วยไลโดซานที่บรรจุด้วยสารเตตราไฮโดรเคอร์คูมินสำหรับการรักษาโรคสะเก็ดเงินเฉพาะที่. ( DEVELOPMENT OF TETRAHYDROCURCUMIN-LOADED CHITOSAN-COATED-NANOSTRUCTURED LIPID CARRIERS FOR TOPICAL TREATMENT OF PSORIASIS) อ.ที่ปรึกษาหลัก : รศ. ภก. ดร.พรชัย โรจนลีทธิศักดิ์, อ.ที่ปรึกษาร่วม : รศ. ดร.ปราณี โรจนลีทธิศักดิ์, ศ. ญ. ดร.โอภา วัชรกุลป์

อนุภาคนาโนตัวพาไขมันที่เคลือบด้วยไลโดซานเป็นอนุภาคนาโนที่มีศักยภาพสูงในการนำส่ง ยาเคมีบำบัดผ่านผิวหนังไปที่มีประสิทธิภาพสูง ในการศึกษาชิ้นนี้ยาค้นแบบที่ใช้ในการพัฒนาสูตรตำรับ คือ เตตราไฮโดรเคอร์คูมิน ซึ่งเป็นเมแทบอลิต์หลักของเคอร์คูมินที่มีคุณสมบัติต้านอนุมูลอิสระ และต้านมะเร็งสูงกว่าเคอร์คูมิน ทั้งนี้ ทำการเตรียมอนุภาคนาโนบรรจุยาต้นแบบโดยวิธีผสมด้วยเครื่องโฮโมจีไนเซอร์แรงเฉือนสูง และปรับสูตรตำรับด้วยวิธีพื้นที่ผิวตอบสนอง เพื่อเพิ่มประสิทธิภาพ การบรรจุเตตราไฮโดรเคอร์คูมินในอนุภาคนาโนตัวพาไขมันที่เคลือบด้วยไลโดซาน พบว่าสูตรตำรับ ที่ปรับให้เหมาะสมมีขนาดอนุภาค  $244 \pm 18$  นาโนเมตร ค่าศักย์ซีต้า  $-17.5 \pm 0.5$  มิลลิโวลต์ ประสิทธิภาพการกักเก็บร้อยละ  $76.6 \pm 0.2$  และการบรรจุยา  $0.28 \pm 0.01$  มิลลิกรัมต่อมิลลิลิตร จากการศึกษาการปลดปล่อยยาในหลอดทดลอง พบว่าอนุภาคนาโนตัวพาไขมันเคลือบด้วยไลโดซาน ปลดปล่อยยาแบบเน้นตามแบบจำลองคอสเมเซอร์-เพบพาส ด้วยกลไกการปลดปล่อยยาที่เป็นการ แพร่แบบฟลักซ์ THC-Ch-NLCs ยากอนุภาคนาโนที่เคลือบด้วยไลโดซานแพร่ผ่านผิวหนังสังเคราะห์ ได้สูงกว่าอนุภาคนาโนที่ไม่ได้เคลือบด้วยไลโดซานอย่างมีนัยสำคัญ เมื่อทดสอบความเป็นพิษต่อเซลล์ไลน์จากผิวหนังมนุษย์ พบว่า อนุภาคนาโนทั้งที่เคลือบและไม่เคลือบด้วยไลโดซานมีความเป็นพิษต่อเซลล์เคียงกัน แสดงให้เห็นว่าอนุภาคนาโนที่เคลือบด้วยไลโดซานเป็นตัวพาที่มีประสิทธิภาพ ในการนำส่งยาผ่านผิวหนัง

จุฬาลงกรณ์มหาวิทยาลัย  
CHULALONGKORN UNIVERSITY

สาขาวิชา เกษศาสตร์และเทคโนโลยี  
ปีการศึกษา 2564

ลายมือชื่อนิติ .....  
ลายมือชื่อ อ.ที่ปรึกษาหลัก .....  
ลายมือชื่อ อ.ที่ปรึกษาร่วม .....  
ลายมือชื่อ อ.ที่ปรึกษาร่วม .....

## 6272004033 : MAJOR PHARMACEUTICAL SCIENCES AND TECHNOLOGY

KEYWORD: Chitosan; Nanostructured lipid carriers; Transdermal delivery;  
Tetrahydrocurcumin; Psoriasis; Cytotoxicity

Hoang Thien Truong : DEVELOPMENT OF TETRAHYDROCURCUMIN-LOADED CHITOSAN-COATED-NANOSTRUCTURED LIPID CARRIERS FOR TOPICAL TREATMENT OF PSORIASIS. Advisor: Assoc. Prof. PORNCHAI ROJSITTHISAK, Ph.D. Co-advisor: Assoc. Prof. Pranee Rojsitthisak, Ph.D., Prof. OPA VAJRAGUPTA, Ph.D.

Chitosan (Ch)-coated nanostructured lipid carriers (NLCs) have great potential for topical delivery with high localization of chemotherapeutics. In this study, tetrahydrocurcumin (THC), a primary metabolite of curcumin with enhanced antioxidant and anticancer properties, was used as a model drug to prepare NLCs. Response surface methodology was employed to optimize THC-loaded Ch-coated NLCs (THC-Ch-NLCs) fabricated by high-shear homogenization. The optimized THC-Ch-NLCs had particle size of  $244 \pm 18$  nm, zeta potential of  $-17.5 \pm 0.5$  mV, entrapment efficiency of  $76.6 \pm 0.2\%$  and drug loading of  $0.28 \pm 0.01$  mg/mL. In vitro release study of THC-Ch-NLCs showed sustained release following the Korsmeyer-Peppas model with Fickian diffusion mechanism. THC-Ch-NLCs demonstrated a significantly higher permeation through the artificial membrane than the THC-NLCs. Furthermore, THC-Ch-NLCs also exhibited cytotoxicity against TNF- $\alpha$ -induced HaCaT cell lines. However, the findings need further investigation to prove that the cytotoxicity is due to the encapsulation of THC in the Ch-NLC since the same effect is also observed in the blank lipid-nanoparticles.



Field of Study:	Pharmaceutical Sciences and Technology	Student's Signature .....
Academic Year:	2021	Advisor's Signature .....
		Co-advisor's Signature .....
		Co-advisor's Signature .....

## ACKNOWLEDGEMENTS

I would like to express my deepest gratitude to my thesis advisor, Associate Professor Pornchai Rojsitthisak, Prof. Opa Vajragupta, Ph.D. and Assoc. Prof. Pranee Rojsitthisak, Ph.D. for their expert advice, invaluable help, and constant encouragement throughout my graduate study. I would also like to sincerely thank the thesis committees for their valuable comments on this thesis.

I would like to acknowledge the Pharmaceutical Research Instrument Center of the Faculty of Pharmaceutical Sciences, Chulalongkorn University for providing the research facilities and instruments. I also thank the staff and my friends at Chulalongkorn University for staying with me and giving me insightful pieces of advice during challenging times.

This work was supported by the Thailand Science Research and Innovation Fund, Chulalongkorn University under Grant CU\_FRB640001\_01\_33\_3 and CU\_FRB65\_heal (56)065\_33\_09 (P.R.). I am thankful to the Ratchadaphiseksomphot Endowment Fund for supporting the Natural Products for Ageing and Chronic Diseases, Chulalongkorn University under Grant GRU 6404733002-1 (P.R.).

Finally, I would like to express my most profound appreciation to my family for their support, encouragement, and inspiration throughout this research. They all kept me working hard, and this thesis would not have been completed without them.

จุฬาลงกรณ์มหาวิทยาลัย  
CHULALONGKORN UNIVERSITY

Hoang Thien Truong

# TABLE OF CONTENTS

	<b>Page</b>
.....	iii
ABSTRACT (THAI) .....	iii
.....	iv
ABSTRACT (ENGLISH).....	iv
ACKNOWLEDGEMENTS.....	v
TABLE OF CONTENTS.....	vi
LIST OF TABLES.....	ix
LIST OF FIGURES .....	x
LIST OF APPENDICES.....	ii
LIST OF ABBREVIATIONS.....	iii
CHAPTER 1 INTRODUCTION.....	1
1.1. Background of the study.....	1
1.2. Rationale and significance.....	3
1.3. Objectives of the study .....	5
1.4. Hypothesis .....	5
CHAPTER 2 LITERATURE REVIEW.....	6
2.1. Psoriasis.....	6
2.1.1. Topical treatment of psoriasis.....	6
2.1.2. TNF- $\alpha$ inhibitors for psoriasis treatment .....	9
2.2. Nanostructured lipid carriers (NLCs) as potential drug delivery system .....	9
2.3. Chitosan as a potential polymer for NLCs .....	14
2.4. Tetrahydrocurcumin .....	17
CHAPTER 3 METHODOLOGY .....	19
3.1. Materials and Instruments.....	19
3.1.1. Materials.....	19

3.1.2. Instruments .....	19
3.2. Methodology .....	20
3.2.1. Drug-excipient compatibility studies .....	20
3.2.2. Preparation of THC-Ch-NLCs .....	20
3.2.3. Optimization of chitosan-coated-nanostructured lipid carriers (Ch-NLCs) containing tetrahydrocurcumin (THC) by Box-Behnken design .....	20
3.2.4. Characterization of THC-Ch-NLCs .....	21
3.2.5. <i>In vitro</i> drug release study of THC from THC-Ch-NLCs .....	22
3.2.6. <i>In vitro</i> skin permeation study through Strat-M <sup>®</sup> membrane .....	23
3.2.7. Cell culture .....	23
3.2.8. Cell viability assay .....	24
3.2.9. Induction of the proliferation of HaCaT cells by TNF- $\alpha$ .....	24
3.2.10. Statistical analysis .....	26
CHAPTER 4 RESULTS AND DISCUSSION .....	27
4.1. Drug-excipient compatibility studies using DSC and FT-IR .....	27
4.1.1. DSC analysis .....	27
4.1.2. FTIR analysis .....	29
4.2. Optimization and data analysis by Design-Expert <sup>®</sup> software .....	30
4.2.1. Model development for particle size, EE, and DL .....	30
4.2.2. Response surface analysis .....	32
4.2.3. Validation of the response surface models .....	35
4.3. Characterization of the optimized formulation .....	35
4.4. <i>In vitro</i> release study of THC from Ch-NLCs and NLCs .....	39
4.5. <i>In vitro</i> skin permeation study through Strat-M <sup>®</sup> membrane .....	42
4.6. Cell viability assay .....	43
CHAPTER 5 CONCLUSION .....	47
APPENDIX 1 .....	48
APPENDIX 2 .....	49
APPENDIX 3 .....	53



REFERENCES .....56  
VITA.....75



## LIST OF TABLES

	<b>Page</b>
Table 1. Various nanoparticulate platforms for the encapsulation of hydrophobic compounds .....	12
Table 2. Studies on Ch-coated NLC formulations.....	15
Table 3. Factors and responses in the Box-Behnken design.....	21
Table 4. Box-Behnken experimental design matrix and response values for the optimization of THC-Ch-NLC formulation.....	31
Table 5. Fit summary of the RSM models.....	35
Table 6. Validation of the prediction capability of the RSM models.....	35
Table 7. Release kinetics of THC from THC-Ch-NLCs and THC-NLCs in pH 7.4 and 5.5.....	41

## LIST OF FIGURES

	<b>Page</b>
Figure 1. Clinical presentations of psoriasis (Armstrong et al., 2020) .....	7
Figure 2. Pathophysiology of psoriasis (Armstrong et al., 2020) .....	8
Figure 3. Chemical structure of chitosan .....	16
Figure 4. Chemical structure of tetrahydrocurcumin.....	18
Figure 5. Drug-excipient compatibility: (A) DSC thermograms of THC, GMS, caprylic triglyceride, THC-GMS, and THC- capric/caprylic triglyceride; and (B) IR spectra of pure THC, lipids, and their binary mixtures.....	28
Figure 6. Response surface plots showing the effects of THC concentration ( $X_1$ ), Ch concentration ( $X_2$ ), and S:L lipid ratio ( $X_3$ ) on (a-c) particle size ( $Y_1$ ), (d-f) EE ( $Y_2$ ), and (g-i) DL ( $Y_3$ ). .....	33
Figure 7. Characteristics of the optimized THC-Ch-NLCs: (A) TEM images at 50,000 and 100,000x magnification); (B) DSC thermograms of THC, Ch-NLC and THC-Ch-NLC; and (C) FT-IR spectra of THC, Ch-NLC and THC-Ch-NLC. ....	38
Figure 8. Cumulative release of unencapsulated THC and THC from THC-NLCs and THC-Ch-NLCs using the dialysis method at (A) physiological (pH 7.4) and (B) tumor microenvironment (pH 5.5); and (C) permeation profiles of THC from THC-Ch-NLCs and THC-NLCs through Strat-M <sup>®</sup> artificial skin membrane .....	39
Figure 9. The viability of HaCaT cells treated with unencapsulated THC and THC-Ch-NLCs containing different THC concentrations .....	44
Figure 10. The viability of TNF- $\alpha$ induced HaCaT cells treated with unencapsulated THC and THC-Ch-NLCs containing different THC concentrations.....	46

## LIST OF APPENDICES

Appendix		Page
1	Calibration curve of THC.....	48
2	DSC thermograms.....	49
3	FT-IR spectra.....	53



## LIST OF ABBREVIATIONS

THC	Tetrahydrocurcumin
Ch	Chitosan
NPs	Nanoparticles
NLCs	Nanostructured Lipid Carriers
Mw	Molecular weight
UV/Vis	Ultraviolet–visible spectrophotometry
FT-IR	Fourier-transform infrared spectroscopy
TEM	Transmission electron microscopes
DLS	Dynamic light scattering
BBD	Box-Behnken design
RSM	Response surface methodology
NaOH	Sodium hydroxide
PBS	Phosphate buffer saline
DMEM	Dulbecco’s modified Eagle’s medium
EE	Encapsulation efficiency
DL	Drug Loading

## CHAPTER 1 INTRODUCTION

### 1.1. Background of the study

Skin is the largest multilayered organ in the human body, accounting for approximately 1.7 to 2.0 square meters. Epidermis, dermis, and subcutaneous tissue are microscopically classified as epithelium (inner layer). The stratum corneum (SC) contains stratified squamous epithelium. This is one of many layers of the stratum granulosum (SG) membrane. SC is divided into nonviable (dead) SC and viable (living) SC. A lipophilic matrix has firmly and efficiently adhered to keratin-filled corneocytes in the SC. The dermis is between 500 and 3,000 mm thick. This includes veins, lymphatics, perspiration glands, and nerve terminals. The subcutaneous adipose layer, situated beneath the skin, has the additional purpose of regulating body temperature and nourishing the organism. This skin barrier helps to limit the permeability of hydrophilic medications, such as pharmaceuticals made of water or glycerin, and it has a part of the SC embedded inside it. However, the viable epidermis is resistant to lipophilic substances ([Bolognia et al., 2012](#), [Montagna et al., 1974](#); [Bartosova et al., 2012](#); [Mbah et al., 2011](#); [Tanwar et al., 2016](#)).

There are at least 100 million people who suffer from psoriasis worldwide, with a prevalence that ranges from 0.09 percent to 11.43 percent depending on the country in which they live. ([World Health Organization., 2016](#)). The scalp, extensor surfaces of the elbows, anterior parts of the lower legs, umbilicus, and natal cleft are all common locations for psoriatic plaques ([Higgins, 2017](#)).

Psoriasis is a chronic skin condition that can harm the patient's quality of life. This disease can strike at any age or gender, and it can strike anyone. Although the

exact origin of psoriasis remains a mystery, it is widely thought to be due to the secretion of cytokines by activated T cells, which result in aberrant keratinization. Psoriasis has been treated using a variety of selective T-cell inhibitors, some of which are FDA-approved. Chronic plaque-type psoriasis, also known as psoriasis Vulgaris, is the most prevalent kind of illness, accounting for around 90 % of all cases. Psoriasis is characterized by keratinocyte hyperproliferation, inadequate differentiation, and inflammation, which manifests clinically in patients as erythematous skin lesions covered by thick silvery scales. (Baliwag et al., 2015; Boehncke et al., 2015).

Many psoriasis therapies suppress the generation of tumor necrosis factor-alpha (TNF- $\alpha$ ), which significantly impacts skin inflammation (Bai et al., 2018). Briefly add the drugs for psoriasis and formulations; hydrophilic or lipophilic drugs.

Chitosan is a biopolymer that has been widely used in the pharmaceutical industry due to its ability to adhere to negatively charged surfaces such as skin and mucosa, bioadhesion (the ability to adhere to negatively charged surfaces such as skin and mucosa), wound-healing properties, and antibacterial activity (Khoushab et al., 2010). Chitosan has been used with solid lipid nanoparticles to improve cellular contact and internalization (Sandri et al., 2010). Other studies have been done using chitosan to improve peptide drug delivery orally (Garcia et al., 2005) and help limit macrophage internalization (Sarmiento et al., 2011; Fonte et al., 2011).

To improve their biopharmaceutical properties, NLCs were coated with chitosan (CS) to achieve an optimal combination of the advantages of lipidic nanoparticles and the biological properties of CS. The goal of this work was to design and develop chitosan-coated nanostructured lipid carriers (Chi-NLCs) encapsulating

tetrahydrocurcumin (THC). The lipid carriers were composed of glycerol monostearate, capric/caprylic triglyceride. The developed formulation aims to be used topically for the treatment of skin hyperproliferative disorders, namely psoriasis. The response surface approach will be used to optimize the nanoparticle formulation, with the Box-Behnken Design as the experimental design, to get the best possible results. The hydrodynamic diameter, encapsulation efficiency, and loading capacity will be evaluated, as well as the Chi-NLCs, which have long-term stability and have enhanced the toxicity of THC *in vitro* against TNF- $\alpha$  induced HaCaT cells when compared to free THC alone.

## **1.2. Rationale and significance**

The conventional solid lipid nanoparticles (SLNs) have previously gotten a lot of interest as a drug delivery system because of the advantages of low toxicity, drug targeting, controlled release, and the ease of being manufactured on a commercial scale. Although SLN is possible for numerous issues to arise depending on the drug, there are still some of the most common downsides including drug leakage during storage and inadequate drug loading. The solid lipid nanoparticle is then combined with the liquid lipid to create NLCs, which results in unique nanostructures with better properties for drug loading, modification of the drug release profile, and stability. The capacity to integrate large amounts of medicines into this type of carrier/delivery system is a key benefit of this NLC delivery system, which is a result of the creation of a less ordered lipid matrix with numerous defects. Because of their unique lipid content and smaller particle size, NLCs maintain tight contact with the stratum corneum, therefore increasing drug flow through the skin. Furthermore, the solidified lipid matrix is feasible to achieve a regulated release of the encapsulated



drug from these carriers. It is possible to integrate significant quantities of medicines into NLCs because they produced a less organized lipid matrix with many defects. A decrease in trans-epidermal water loss has also been shown to significantly enhance skin hydration and exhibit occlusive characteristics, which means they have occlusive capabilities (Jana et al., 2009).

These carrier systems circumvent the limits of traditional SLN and more fluid lipid DDS, which have been reported in the past. Solid particles, as opposed to liposomes and emulsions, have several benefits, including the ability to preserve integrated active chemicals from chemical degradation and the ability to modulate the release of the substance over these other delivery systems. It is about finding different kinds of lipid-based nano systems, their structure and characteristics, as well as their various levels of stability, and how they may be used to aid drug administration (Anthony et al., 2012).

The administration of lipid-based drug delivery systems can be accomplished by several routes including oral, parenteral, ophthalmic, intranasal, dermal/transdermal, and vaginal (LBDDS). It is also regarded as the technique of administering drugs for chronic treatments, according to some experts. At the beginning of the development, a reasonable and methodical strategy is required to design a formulation that prevents unpredictable and poor correlations *in vitro/in vivo*. Several writers have provided several important suggestions on routes and formulation techniques, all of which are highly recommended (Hina et al., 2014). The chitosan-NLC combines the benefits of NLC with the biological characteristics of chitosan to create a unique product. In addition, the bio adhesion characteristics of chitosan can help to keep drugs at the site of application for long periods. Aside from

that, the antibacterial activity of chitosan is promising for the treatment of skin disorders (Khoushab et al., 2010). There are no studies on THC-loaded chitosan-coated nanostructured lipid carriers. The mechanisms of action such as drug loading capacity, drug release, cytotoxicity, and cellular uptake have not been clearly studied yet (Daniela et al., 2011; Leticia et al., 2019).

### 1.3. Objectives of the study

This study aimed to:

- a. Prepare, optimize and characterize chitosan-coated-nanostructured lipid carriers (Chi-NLCs) loaded with tetrahydrocurcumin (THC).
- b. Determine the release profile and permeation of the optimized THC-loaded Chi-NLCs through the artificial skin.
- c. Evaluate the effectiveness of the optimized THC-loaded Chi-NLCs against TNF- $\alpha$ -induced HaCaT cells.

### 1.4. Hypothesis

The developed chitosan-coated-nanostructured lipid carriers (Chi-NLCs) can be used as an effective delivery system of tetrahydrocurcumin (THC) and other bioactive compounds for the enhancement of cytotoxicity against TNF- $\alpha$ -induced HaCaT cells through topical administration.

## CHAPTER 2 LITERATURE REVIEW

### 2.1. Psoriasis

#### 2.1.1. Topical treatment of psoriasis

There are several multiple causes for psoriasis. A mild case may have a few isolated inflammatory skin lesions, whereas a severe case may have extensive plaques covering more than 10% of the body surface area (Figure 1) ([Hawkes et al., 2017](#)). The exact cause of psoriasis and the pathophysiology of the disease is yet unexplained (Figure 2). At this time, there is no cure for psoriasis, and only palliative therapy options are available. To successfully manage psoriatic symptoms, patients must have a diagnosis of psoriasis and the condition must be severe. In mild cases of psoriasis, topical treatments are utilized; phototherapy and systemic therapy, on the other hand, are reserved for moderate to severe cases of the disease, according to the American Academy of Dermatology ([Woo et al., 2017](#)).

Topicals are commonly utilized in the treatment of psoriasis and are considered to be the basis of the disease. Many topicals are available, however, there are no worldwide consensus criteria for determining the best method of use. Doctors should use information from randomized controlled trials (RCTs), patient outcomes, and patient preferences to make clinical decisions. During five years from 2007 to 2012, Maruani et al. conducted an extensive assessment of RCTs on topical psoriasis medications and determined that just a few RCTs exist. Instead of a two-arm experiment with an inactive control arm, an inactive control was chosen as the preferable comparator. The latter was the case in 13 (22%) instances ([Maruani et al., 2015](#)).

The psoriasis topical therapy is evolving. In nations where calcipotriol/betamethasone dipropionate cutaneous foam has been distributed, the therapeutic choices for topical treatment have been broadened significantly. Adherence to therapy may be improved with better formulations. It has also recently been shown that Crisaborole<sup>®</sup>, which is authorized for the treatment of atopic dermatitis, may have a significant influence on the treatment of the condition in the future (Hashim et al., 2019).



**Figure 1.** Clinical presentations of psoriasis (Armstrong et al., 2020)

Treatment options for psoriasis now include conventional therapy (topical, systemic, and phototherapy), biologics, and immunotherapy (Rapalli et al., 2018). Several alternative treatments for mild psoriasis include vitamin D analogs, calcineurin inhibitors, retinoids, coal tar, emollients, and corticosteroids. Using a topical application has been linked to the most often reported side effects of skin irritation and atrophy (Rapalli et al., 2018; Torsekar et al., 2017).

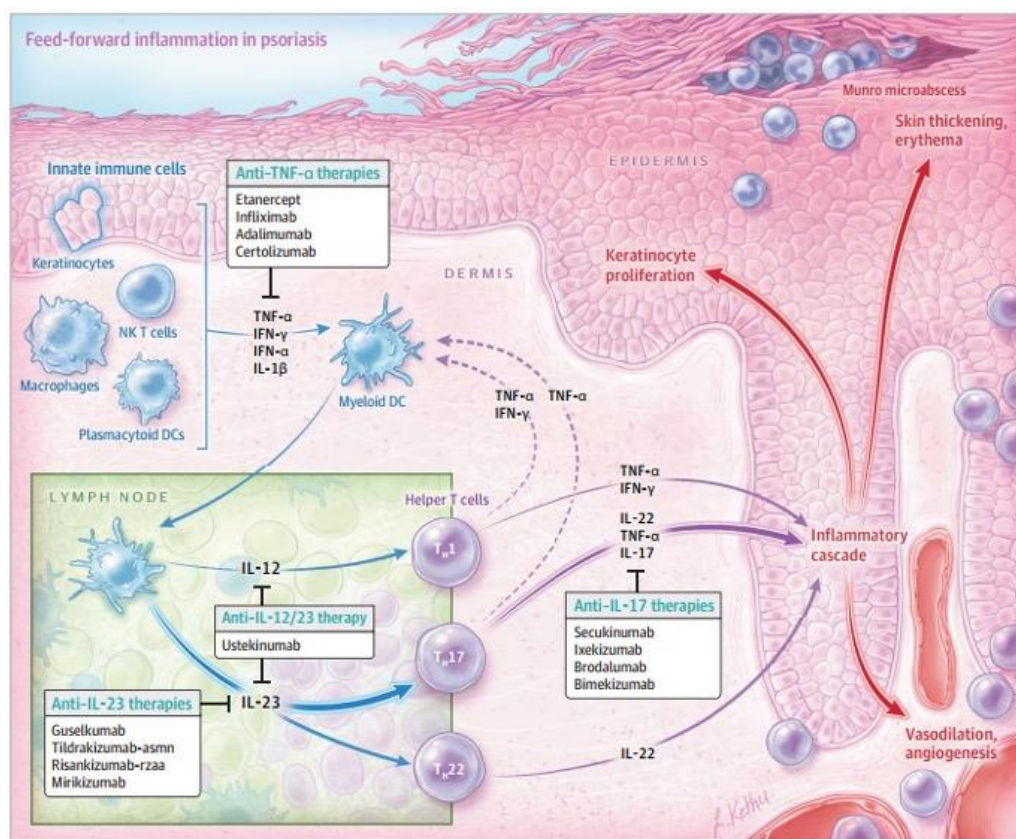


**Figure 2.** Pathophysiology of psoriasis (Armstrong et al., 2020)

Patients with severe psoriasis are administered oral-systemic medications such as methotrexate, acitretin, and cyclosporine, among other things. The immunosuppressive and anti-inflammatory properties of these medicines are the methods through which they work (Meng et al., 2018).

### **2.1.2. TNF- $\alpha$ inhibitors for psoriasis treatment**

When TNF- $\alpha$  is produced by T cells and antigen-presenting cells (APC) in psoriatic skin, it is referred to as proinflammatory cytokine (Baliwag et al., 2015). HaCaT cells release more signaling pathways, including MAPKs, NF- $\kappa$ B, and caspases (Kim et al., 2015; Nedoszytko et al., 2014).

TNF-inhibitors, such as adalimumab, etanercept, and infliximab, are biologics that work by inhibiting the cytokine TNF's ability to cause inflammation (Tobin et al., 2005). One study found that TNF-inhibitors did not affect people with chronic kidney disease. The varied genetic origins of the patients might be a contributing factor to the modest curative responses (Baliwag et al., 2015). To cover the high costs of biologics manufacture, patients are forced to take the medication for the long term, which prevents them from obtaining more of it because of cost (Tonel et al., 2009; Kelly et al., 2015).

When moderate to severe psoriasis and psoriatic arthritis has already developed, TNF- $\alpha$  inhibitors might be considered an option for the patient who is no longer appropriate for conventional therapy (Tobin et al., 2005; Wcislo-Dziadecka et al., 2016). Combination therapy is often superior to monotherapy since it improves efficacy and has fewer adverse effects.

## **2.2. Nanostructured lipid carriers (NLCs) as potential drug delivery system**

Conventional formulation techniques may no longer be sufficient to achieve adequate bioavailability and specific clinical characteristics as the number of poorly soluble chemical entities from drug development rises. Advances in drug delivery technologies, such as lipid-based drug delivery systems (LBDDS), have become crucial in creating novel chemical entities in modern molecular pharmaceuticals. Lipid-

based drug delivery systems (LBDDS) are a category of technologies that employ lipid molecules, either alone or in conjunction with other biocompatible materials, to deliver pharmaceuticals in a more compatible way with biological systems. Lipid-based drug delivery systems are considered the most suitable carriers for improving solubility and enhancing the efficacy of hydrophobic and lipophilic medicines (Anurag et al., 2015).

Nano-based carriers, such as lipid-based, polymeric, inorganic, bio-inspired, and hybrid nanoparticles, have unique characteristics, such as precise targeting of malignant cells, minimizing side effects, and developing trends in multi-drug resistance in dermal and transdermal drug delivery systems, among others (Sutradhar et al., 2014). Biodegradable, non-toxic, and non-irritant lipid nanocarriers outperform traditional drug delivery systems in various ways. It is possible to attach lipid nanocarriers to the lipid film of SC because of their small size (ranging between 40 and 800 nm). This enables more drug molecules to permeate into deeper layers of the skin. Besides that, they show the occlusion effect, which enhances skin moisture and, consequently, improves medication absorption (Montenegro et al., 2016; Wissing et al., 2003; Soma et al., 2017).

The conventional solid lipid nanoparticles (SLNs) have previously gotten a lot of interest as a drug delivery system because of the advantages of low toxicity, drug targeting, controlled release, and the ease of being manufactured on a commercial scale. Although SLN is possible for numerous issues to arise depending on the drug, some of the most common downsides include drug leakage during storage and inadequate drug loading. The solid lipid nanoparticle is then combined with the liquid lipid to create NLCs, which results in unique nanostructures with better properties for

drug loading, modification of the drug release profile, and stability. The ability to integrate large amounts of medicines into this type of carrier/delivery system is a key benefit of this NLCs delivery system, which creates a less ordered lipid matrix with numerous defects. Because of their unique lipid content and smaller particle size, NLCs maintain tight contact with the stratum corneum, therefore increasing drug flow through the skin. Furthermore, the solidified lipid matrix is feasible to achieve a regulated release of the encapsulated drug from these carriers. It is possible to integrate significant quantities of medicines into NLCs because they produced a less organized lipid matrix with many defects. A decrease in trans-epidermal water loss has also been shown to significantly enhance skin hydration and exhibit occlusive characteristics, which means they have occlusive capabilities. ([Jana et al., 2009](#)).

These carrier systems circumvent the limits of traditional SLN and more fluid lipid DDS, which have been reported in the past. Solid particles, as opposed to liposomes and emulsions, have several benefits, including the ability to preserve integrated active chemicals from chemical degradation and the ability to modulate the release of the substance over these other delivery systems. It is about finding different kinds of lipid-based nanosystems, their structure and characteristics, as well as their various levels of stability, and how they may be used to aid drug administration ([Anthony et al., 2012](#)).

Developed in 1999 ([Müller et al., 2002](#); [Beck et al., 2011](#)), lipid nanoformulations would be classified as the second generation (nanostructured lipid carriers, NLCs). According to [Müller et al. \(2002\)](#), NLCs were first used to incorporate retinol, which is a chemical that degrades when exposed to oxidizing agents or light. Many further studies have been conducted to establish the suitability



of NLCs as drug carriers for a wide range of medications (Beloqui et al., 2016). NLCs may be used to encapsulate drug molecules for delivery via a variety of routes, including oral (Zhang et al., 2011; Tran et al., 2014; Chen et al., 2010; Beloqui et al., 2014), intravenous (e.g., artemether) (Li et al., 2010; Shi et al., 2013). For cutaneous and transdermal administration, examples of medicines in the form of NLCs may be found here.

**Table 1.** Various nanoparticulate platforms for the encapsulation of hydrophobic compounds

Formulation	Method for preparation	Result	Reference
Nanoparticles	Emulsion polymerization interfacial polymerization	Similar cytotoxicity to co-administration, higher cytotoxicity than free drug, improve the efficacy	Jinhua et al., 2012.
Niosomes	Amphiphilic self-assembly and thin-film hydration method	Higher cytotoxicity when compared to free drugs	Varsha et al., 2015
Polymeric micelles	Co-solvent evaporation	Exhibited desirable anti-cancer activity, pH sensitive micelles	Thisirak et al., 2017.
Lipid nanoparticles	High-pressure microfluidics technique	Enhanced permeability and retention effect	Xiaojing et al., 2015.
Solid lipid nanoparticles	Micro emulsification method 82–85 °C	Significantly better (p 0.001) activity than free THC in gel	Vandita et al., 2018.
Nanostructured lipid carriers (NLCs)	Emulsion evaporation and solidification at a low T 75°C	NLC presented improved drug loading capacity which increased with increasing the liquid lipid content	Le-Jiao et al., 2010.
Nanostructured lipid carriers (NLCs)	High-pressure homogenization technique (85 °C)	Possibly minimize its systemic access and side effects	Bharti et al., 2015.
Nanostructured lipid carriers (NLCs)	Emulsion evaporation	Higher anticancer activity, apoptosis rate compared to that of native curcumin	Fengling et al., 2017.

More drug entrapment efficiency in NLCs has been claimed to be a consequence of defects in the NLCs structure, increased area for drug loading, and the existence of both solid and liquid lipids, in which many medicines have greater solubility (Poonia et al., 2016; Park et al., 2017; Natarajan et al., 2017).

Drug loading capacity (DLC) NLCs is designed to compensate for SLN problems in the following ways: they lower the risk of drug ejection during storage, reduce the high-water content in SLN dispersion, and allow for improved drug loading capacity (Montenegro et al., 2016; Beloqui et al., 2016; Purohit et al., 2016). An unilayered lipid film is produced on the skin due to NLCs administration, resulting in the constriction of blood vessels in the affected area. It is possible to reduce water evaporation, which leads to improved moisture of the skin, and thus to promote drug permeation through the SC. Aside from that, the presence of surfactants in NLCs causes structural modifications to be induced in the skin, and it also acts as a skin permeable activator (Beloqui et al., 2016; Yousef et al., 2017). In this study, nanoparticles (NLCs) with a diameter less than 400 nm and a concentration of at least 35 percent high crystallinity lipid had the largest obstruction impact, being 15 times more occlusive than microparticles in the same study (Purohit et al., 2016; Kamble et al., 2012; De Vringer et al., 1997).

The method of drug delivery may affect the amount of the medication that gets through the NLCs when applied topically. Such factors as the type and quantity of lipids and surfactants, as well as the position of the drug inside the NLCs, might affect penetration. Because NLCs alter intercellular packing, the result is a decrease in corneocyte structure as well as an increase in the number of spaces between corneocytes. The two processes by which medicines are released from NLCs in the

body are diffusion and lipid particle disintegration (Beloqui et al., 2016; Purohit et al., 2016).

### 2.3. Chitosan as a potential polymer for NLCs

Polymeric nanoparticles have recently caught the public's curiosity as a potential component of nano-drug targeting systems that add the drawbacks of synthetic polymers. The biological characteristics of naturally occurring polymers, such as chitosan, which are non-immunogenicity, low cytotoxicity, biocompatible, sustained-releasing, and high drug encapsulating efficiency make them appealing for drug carriers (Parveen et al., 2015).

The types of nanoparticles are classified into five major categories based on the method of fabrication: lipid-based (liposome, lipoplex, solid lipid nanoparticle), polymeric (micelle, polymersome, nanocapsule, nanosphere, dendrimer, nanogel, nano complex), inorganic (gold nanoparticles, magnetic nanoparticles, silica nanoparticles, quantum dots, carbon nanomaterial) (Yin and Zhong., 2020). Nanoparticles with a polymeric composition, such as polymeric nanoparticles (polymeric NPs), may offer the most effective approach for delivering cancer medications through the circulatory system. Preclinical studies and clinical trials have thus far explored polymeric NPs. According to Schäfer-Korting (2010), these polymeric NPs may be easily produced by combining biodegradable polymers with nonbiodegradable polymers. Microbial fermentation polymers (poly hydroxybutyrate) can be grouped with other polymers based on their natural origin (starch, cellulose, protein, alginate, chitosan), or their synthetic origin (polylactic acid (PLA), polycaprolactone (PCL), poly (lactic-co-glycolic acid) (PLGA), polyvinyl alcohol (PVA), polyethylene glycol (PEG) (Yu et al., 2006). Among these natural polymers,

cationic chitosan is noteworthy materials for the construction of nanoparticle-based vehicles because of their excellent biological features, which include non-toxicity, biocompatibility, non-immunogenicity, biocompatibility, adsorption enhancer, and protective effects (Chellat et al., 2005; Coppi et al., 2009; Jayakumar et al., 2010; Shukla et al., 2012).

**Table 2.** Studies on Ch-coated NLC formulations

Formulation	Method	Materials	Reference
Nanostructured lipid carriers (NLCs) dual-responsive hydrogel carboxymethyl chitosan	Melt-emulsification combined with ultrasonication technique 87°C	Compritol 888 ATO (solid lipid), MCT (liquid lipid), Cremophor EL (surfactant) and soy lecithin (surfactant), 127 and CMCS	Yibin et al., 2017.
Chitosan as coating for NLCs skin delivery fucoxanthin	High shear homogenization hydrochloride, soluble in an aqueous environment	Bacuri butter Tucumã oil Polysorbate 80 and sorbitan monooleate Chitosan (CS)	Leticia et al., 2019.
Chitosan-coated nanostructured lipid carriers (Ch-NLCs) Simvastatin as co-adjuvant treatment of melanoma	Hot high-pressure homogenization technique	Precirol® ATO Squalene Tween® 80	Antonella et al., 2019.

The cationic natural polysaccharide chitosan (CS) is composed of  $\beta$ -(1-4)-glycosidic linked between D-glucosamine and N-acetyl-D-glucosamine (Figure 3) (Lertsutthiwong et al., 2011; Prabakaran et al., 2008). Chitosan is commercially obtained by deacetylation or degradation of chitin, which is commonly derived from fungi cell walls and insect bodies (Motiei et al., 2017). There are also significant effects on CS breakdown, crystallinity, surface charge, and cellular responsiveness due to the molecular weight and degree of deacetylation (Yuan et al., 2011). The

human internal enzyme lysozyme, in particular, can break down CS into monosaccharides and oligosaccharides that may be taken by the body and used (George et al., 2006). Its unique biological and physicochemical properties are biodegradability, biocompatibility, non-toxicity, mucoadhesion, gelling, cellular activity, and controlled drug release. Chitosan can be synthesized in a variety of forms, including beads, films, micro-and nanoparticles; it can also be fabricated into various other forms. Because of these applications in pharmaceutical and medicinal fields, such as tissue regeneration, cosmeceutical manufacturing, tissue regeneration, drug and vaccine delivery systems (Xiao et al., 2018; Yan et al., 2018; Martinez-Martinez et al., 2018), CS has been used in a variety of pharmaceutical and medical fields.

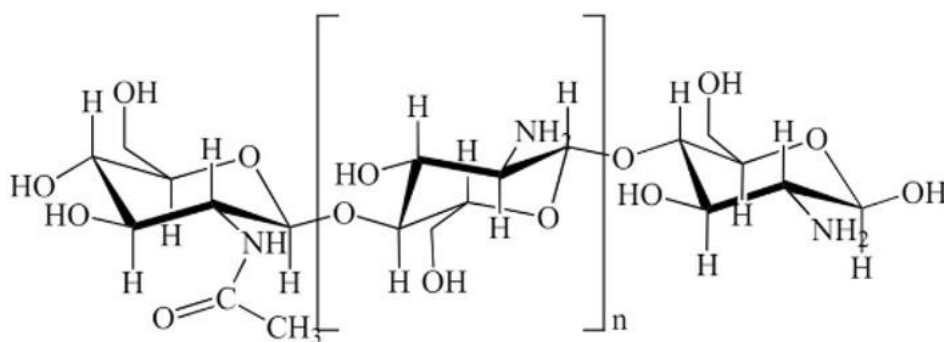


**Figure 3.** Chemical structure of chitosan

Furthermore, chitosan (CS), a cationic polysaccharide derived from glucosamine and N-acetylglucosamine and obtained by fractional deacetylation of chitin (Duan et al., 2010; Sailaja et al., 2010; Zhang and Kawakami, 2010), possesses several properties that are important in skin diseases: it can enhance coagulation by both hemagglutininations (Sandri et al., 2011; Jayakumar et al., 2010; Manivasagan et

al., 2017). Furthermore, it accelerates the remodeling process while simultaneously boosting angiogenesis.

#### 2.4. Tetrahydrocurcumin

Tetrahydrocurcumin (THC), a curcumin metabolite that is believed to be helpful for local therapies in the gut, is a substance that has been studied extensively (Nakamura et al., 1998; Osawa et al., 1995; Pan et al., 1999). Additionally, it is a colorless antioxidant molecule with exceptional stability at physiological pH (7.4) (Plyduang et al., 2014) and in plasma and is a powerful antioxidant agent. Furthermore, THC has been shown to have superior anti-inflammatory properties to curcumin (Plyduang et al., 2014). Even if a few studies suggest that THC is used in cosmetic formulations as a depigmenting agent, it is still an understudied chemical for topical diseases (Muhammad et al., 2010). As a result of its low water solubility (0.0056 mg/mL) and log P value of 2.98, THC is anticipated to be a poor skin permanent because of its low aqueous solubility (0.0056 mg/mL) (Figure 4) (Saipin et al., 2011; Denis et al., 2005).

THC, one of the primary metabolites of curcumin, has the same pharmacological characteristics as curcumin and is used to treat various diseases. THC is insoluble in water, although it is soluble in ethanol, glacial acetic acid, and other solvents. Because of THC's poor water solubility, it has limited pharmacological activity. Furthermore, a relatively short stomach emptying time may result in an insufficient release of THC from the dosage form at the absorption site, resulting in a reduction in the efficiency of the dose that has been given (Anurag et al., 2015). Curcumin helps regulate various inflammatory cytokines, including IL-1 $\beta$ , IL-6, IL-12, TNF alpha, and IFN gamma, as well as JAK-STAT, AP-1, and NF-kappaB signal

transduction pathways in immune cells. However, using pure active substances like curcumin at greater dosages for medicinal reasons requires considerable care (Bright., 2007). Both humans and rats have had THC found in their digestive tracts and hepatocyte cytosol. A reductase enzyme located in the cytosolic segment of either intestinal or liver cells was suggested to convert curcumin into THC. The anticancer and anti-angiogenic effects of THC and its ability to prevent type II diabetes have also been shown. Azoxymethane-induced colon carcinogenesis has also been shown to be more effective than curcumin in this regard. As a result of its low solubility in water and poor gastrointestinal absorption, THC is classified as a BCS class IV medication. According to the current research, the medicinal potential of THC may be accomplished via the use of NLCs formulations, which have a higher bioavailability than traditional pharmaceuticals. A primary aim of the current research is creating a THC nanostructured lipid carrier with increased bioavailability.

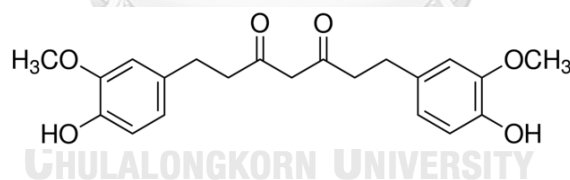


**Figure 4.** Chemical structure of tetrahydrocurcumin

## CHAPTER 3 METHODOLOGY

### 3.1. Materials and Instruments

#### 3.1.1. Materials

The following chemicals, specifications and suppliers were used for the study: tetrahydrocurcumin, tween 80, poloxamer 407, glycerol monostearate, capric/caprylic triglyceride, sodium heparin, keratinocyte cell line (HaCaT cell line), chitosan (MW=75 kDa, 91.74% DD), dimethyl sulfoxide (DMSO), glacial acetic acid, sodium hydroxide, sodium acetate buffer, PBS (pH 7.4) (Sigma-Aldrich, USA), deionized water, and ultra-pure water.

#### 3.1.2. Instruments

The following instruments, and their respective models and brands, were provided by the Faculty of Pharmaceutical Sciences: Homogenizer yellow line DI 18 basic, intersil® ODS- 3 (4.6 x150 mm, 5 $\mu$ ) column, UV-Vis spectrophotometer (Agilent Carry 60), zetasizer (Malvern Nano ZS), ultracentrifuge (Hitachi CP 100NX), incubator shaker (MaxQ 6000 shaker), magnetic stirrer with hotplate (Thermolyne, USA), vortex mixer, dialysis regenerated cellulose membrane (MWCO 10-14 kDa), analytical balance, lyophilizer, microplate reader (Infinite 200 PRO), confocal fluorescence microscope (Zeiss Apotome 3). The Fourier-transform infrared spectroscopy (FT-IR) and scanning calorimetry (DSC) were performed by the Scientific and Technological Research Equipment Center of Chulalongkorn University and NMR laboratory of the Faculty of Pharmaceutical Sciences, respectively.



## **3.2. Methodology**

### **3.2.1. Drug-excipient compatibility studies**

The compatibility study of THC with two lipids, including GMS and capric/caprylic triglyceride, was evaluated using Differential Scanning Calorimetry (DSC 204 F1 Phoenix®, NETZSCH, 95100 Selb, Bavaria, Germany) at a heating rate of 10 °C/min from 30 °C to 400 °C in a dynamic nitrogen environment. The Fourier transform infrared (FT-IR, PerkinElmer Inc., Boston, MA) spectra of each compound were scanned from 400-4000 cm<sup>-1</sup>.

### **3.2.2. Preparation of THC-Ch-NLCs**

For efficient melting and mixing, an ethanolic solution of THC (25 mg/mL) was added to a mixture of solid and liquid lipid at a ratio of 7:3 (5% w/w) and heated at 75±5 °C. Meanwhile, an aqueous phase containing Tween 80 (1% w/w) was heated at the same temperature before adding into the melted oleaginous phase. The resulting emulsion was stirred continuously for 5 min at a constant temperature of 75±5 °C and subjected to high-shear homogenization for 10 min at 8000 rpm. The emulsion was cooled down to room temperature and equilibrated in dark for 24 h. A 20 mL of Ch in glacial acetic acid (1% v/v) was then added dropwise to 100 ml of THC-NLCs with continuous mixing for 30 min. The obtained emulsion was stored in dark for 24 h. Finally, THC-Ch-NLCs were adjusted to pH 5.4 by adding approximately 500 µL of an aqueous NaOH solution (20% w/v).

### **3.2.3. Optimization of chitosan-coated-nanostructured lipid carriers (Ch-NLCs) containing tetrahydrocurcumin (THC) by Box-Behnken design**

A three-factor, three-level Box-Behnken design was employed to generate and randomized experimental conditions and construct the polynomial models to optimize

THC-Ch-NLCs. The effects and interactions of the concentration of THC ( $X_1$ ), the percentage of Ch ( $X_2$ ), and the solid-to-liquid lipid ratio ( $X_3$ ) on the particle size ( $Y_1$ ), encapsulation efficiency (EE,  $Y_2$ ), and drug loading (DL,  $Y_3$ ) were evaluated. The experimental range of the factors and the constraints of the responses are shown in Table 3.

**Table 3.** Factors and responses in the Box-Behnken design

Variables	Levels used		
	Low	Medium	High
<b>Factors:</b>			
$X_1$ = THC (mg/mL)	5	15	25
$X_2$ = Ch (% w/v)	0.05	0.1	0.2
$X_3$ = Solid: Liquid Lipid ratio	3:7	5:5	7:3
<b>Responses:</b>			
	Constraints		
$Y_1$ = Particle size (nm)	Minimize		
$Y_2$ = EE (%)	Maximize		
$Y_3$ = DL (%)	Maximize		

### 3.2.4. Characterization of THC-Ch-NLCs

The mean particle size, polydispersity index (PDI), and zeta potential were determined using a Zetasizer (Nano-ZS, Malvern Instruments, UK). Each sample was diluted 400x with ultrapure water and was analyzed in triplicates. The morphology of the THC-Ch-NLCs was determined by Transmission electron microscopy (TEM, Model JEM-2100, JEOL, Tokyo, Japan). Each sample was prepared by diluting 500x with filtered ultrapure water. The diluted NLCs were loaded onto the copper grids and allowed to dry in a desiccator for 24 h before imaging.

The EE and DL were computed by quantifying the unencapsulated THC from the supernatant after ultracentrifugation at a speed of  $105,000 \times g$  at 4 °C for 45 min. The absorbance of the supernatant was analyzed using a UV-Vis spectrophotometer

(Agilent Carry 60, Agilent Technologies, CA 95051, USA) at 281 nm, and the amount of THC was calculated against the THC standard curve ( $y=0.054x+0.0364$ ;  $R^2=0.9996$ ). The collected NLCs were lyophilized for 24 h and weighed accurately. The EE and DL were calculated using Eq. (1) and Eq. (2), respectively:

$$EE (\%) = (W_1 - W_2) / W_1 \times 100\% \quad (1)$$

$$DL (\%) = (W_1 - W_2) / W_3 \times 100\% \quad (2)$$

Where  $W_1$  is the weight of the initial THC added to the formulation,  $W_2$  is the weight of free THC quantified from the supernatant, and  $W_3$  is the weight of the lyophilized THC-Ch-NLCs.

### 3.2.5. *In vitro* drug release study of THC from THC-Ch-NLCs

The dialysis method was used to evaluate the *in vitro* release of THC from THC-Ch-NLCs. Firstly, a dialysis bag with a molecular cut-off of 12,000 Da was pre-soaked in the medium before the experiment. A phosphate-buffered saline (PBS) solution (1 mg/mL potassium dihydrogen phosphate, 2 mg/mL dipotassium hydrogen phosphate, 8.5 mg/mL sodium chloride in deionized water, pH 7.4) was prepared as a medium to mimic physiological pH, while sodium acetate buffer (50 mg/mL sodium acetate in 1% acetic acid, adjust the pH with 4.2 g/L sodium hydroxide to pH 5.5) was prepared to mimic the tumor microenvironment pH. Each bag was filled with 20 mL of THC-Ch-NLCs or THC-NLCs and sealed on both sides with dialysis clips. The sealed bag was fully immersed in 500 mL of the medium containing ethanol (30 % v/v) while stirring at 600 rpm at 37 °C. An aliquot of the medium was collected at various time points (0.25, 0.5, 1, 2, 4, 6, 8, 12, 24, 36, and 48 h) and replaced with the same volume of fresh medium. THC in the collected samples was quantified by UV-Vis

spectrophotometry at 281 nm and calculated against the calibration curve. The % cumulative drug released was computed using Eq. (3):

$$\text{Cumulative release (\%)} = (\text{THC released}) / (\text{THC formulation}) \times 100 \quad (3)$$

Mathematical models for the evaluation of drug release kinetics (zero order, first order, Peppas-Korsmeyer, and Hixson-Crowell) were fitted to the data using DD solver software, Microsoft Excel Plugin Program (Zhang et al., 2010). The best-fit model was selected based on the highest adjusted R<sup>2</sup>, MSC values, and the lowest AIC (Barzegar-Jalali, 2008).

### **3.2.6. *In vitro* skin permeation study through Strat-M<sup>®</sup> membrane**

To ensure successful delivery of THC-Ch-NLCs, *in vitro* skin permeation study using Franz cell diffusion assay was conducted. Strat-M<sup>®</sup> was used as an artificial membrane to mimic human skin. The membrane was mounted onto the Franz-cell and hydrated with PBS (pH 7.4) for 30 min at a constant temperature at 37 °C. The sample (equivalent to 0.13 mg/mL of THC) was loaded into the donor compartment. An approximately 300 µL of the receptor medium was collected at different time points (0.25, 0.5, 1, 2, 4, 6, 8, 12, 24, 36, and 48 h) and replaced with the same volume of fresh medium. THC in the collected samples was quantified by UV-Vis spectrophotometry at 281 nm against the calibration curve. The total amount of THC that permeated through the membrane was calculated and plotted against time. The permeation kinetics of THC-Ch-NLCs were finally determined.

### **3.2.7. Cell culture**

The immortalized HaCaT human keratinocytes were cultured in 75 cm<sup>2</sup> flasks with Dulbecco's modified Eagle's medium (DMEM) supplemented with 10% fetal

bovine serum (FBS), 100 U/mL penicillin, and 100 mg/mL streptomycin. Cultured flasks were maintained at 37°C with 95% air and 5% CO<sub>2</sub> in the humidified incubator. The medium was replaced every 3-4 days, and cells were sub-cultured by trypsin treatment once a week.

### 3.2.8. Cell viability assay

Using 3-(4,5-dimethylthiazol-2-yl)-2, 5-diphenyltetrazolium bromide tetrazolium (MTT) assay, the effect of the nanoformulations on the viability of HaCaT cells was evaluated. The HaCaT cells in culture media were seeded in a 96-well plate with a density of  $5 \times 10^3$  cells/well and incubated for 24 hours at 37 °C with 95% air and 5% CO<sub>2</sub> incubator until they reached 70-80 % confluence. Afterward, the cultured cells were washed with serum-free media. HaCaT cells were treated with 0.5% (v/v) DMSO as control and pure THC, blank Ch-NLCs, and THC-loaded Ch-NLCs as the treatment groups. The treated cells were incubated for 24 hours and carefully washed with PBS. Then MTT reagent (0.5 mg/mL in PBS) was added to each well and incubated in a humidified incubator for 4 hours. The medium was discarded and replaced with DMSO to dissolve the insoluble formazan crystals in the cell culture. The absorbance was measured at a 540 nm microplate reader to confirm the results. The cell viability (%) was computed using Eq. (4):

$$\text{Cell viability (\%)} = (\text{OD Sample}) / (\text{OD Control}) \times 100 \quad (4)$$

### 3.2.9. Induction of the proliferation of HaCaT cells by TNF- $\alpha$

The immortalized human epidermal keratinocytes cell line (HaCaT) was used as a model system to investigate the anti-psoriatic efficacy of the THC-loaded Ch-NLCs formulation. Psoriasis is a chronic skin condition characterized by an aberrant

cell death state. Tumor necrosis factor TNF- $\alpha$  is a critical cytokine in the development of psoriasis, and TNF- $\alpha$  stimulated HaCaT cells have been used as a psoriasis model system to study the expression of psoriasis-associated genes in humans (Pattarachotanant et al., 2014). To obtain HaCaT cells, seed the cells at a density of  $5 \times 10^3$  cells per 200  $\mu$ L of DMEM (containing 10% v/v heat-inactivated fetal bovine serum and 1% (v/v) penicillin-streptomycin) at 37 °C in a humidified air atmosphere containing 5% CO<sub>2</sub>.

A total of 24 hours was spent treating the cell groups with seeding, followed by washing with the serum-free medium before being seeded with TNF- $\alpha$  at a final concentration of 10ng/mL for a 24-hour incubation. In the experiment, the cells were washed with the serum-free medium before being incubated with pure THC, blank Ch-NLCs, THC-loaded Ch-NLCs concentrations of 0.05 and 0.1  $\mu$ g/mL of the total THC concentration, respectively. In addition, a control experiment was conducted to determine whether the THC treatment had any anti-psoriatic effects. The final DMSO concentration in each of the treatment groups was 0.5 % (v/v). DMSO was added to serum-free medium to provide accurate control for cells growth. After 24 hours of incubation, the cells were washed with a serum-free medium. They then added to a solution of 3-(4, 5-dimethylthiazol-2-yl)-2, 5-diphenyltetrazolium bromide (MTT) (final concentration of 0.5 mg/mL) to detect the presence of MTT from the cells were tested to determine their viability after an additional 4 hours. To dissolve the formazan crystals, the final solution was taken out of the microplate wells and mixed with DMSO to create a solution. A microplate reader was used to detect absorbance at 540 nm, which was obtained after the crystals were dissolved and the solution had been withdrawn from the wells (Gomez et al., 2019; Yunyun et al., 2021).

Each sample was tested four times in total. The number of viable cells in the group that received TNF- $\alpha$  concurrently with the other groups was compared to the number of viable cells in the group that did not receive TNF- $\alpha$ .

### **3.2.10. Statistical analysis**

All experiments were performed with at least three independent replicates and data were expressed as mean  $\pm$  standard deviation. The RSM models were generated using multiple linear regression and analyzed with one-way ANOVA using the Design-Expert<sup>®</sup> software 13.0.5.0 (Stat-Ease, Inc., Minneapolis, MN, USA). The percentage cell viability was analyzed using two-way ANOVA with Tukey HSD as the pairwise comparisons test. All statistical parameters of the cellular assays were analyzed using GraphPad<sup>®</sup> Prism software 9.3.0 (San Diego, CA, USA). P-values < 0.05 were considered statistically significant.

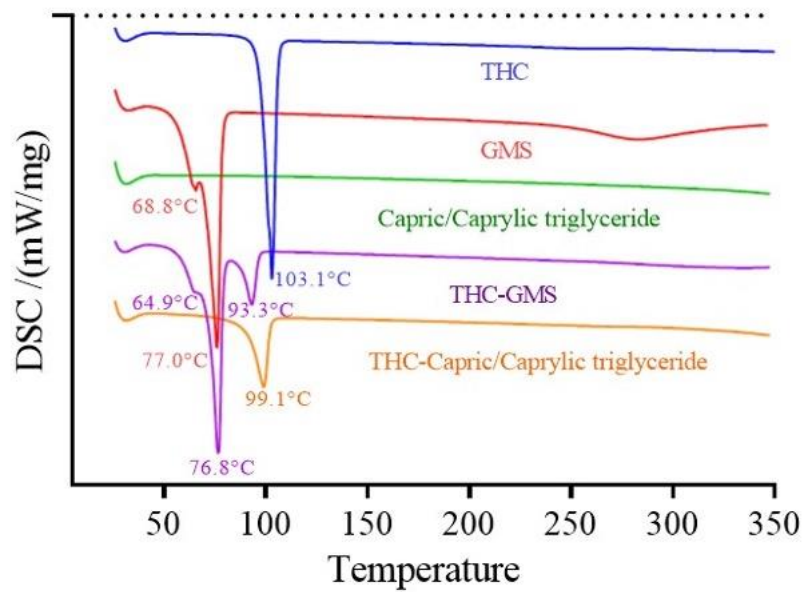
## CHAPTER 4 RESULTS AND DISCUSSION

### 4.1. Drug-excipient compatibility studies using DSC and FT-IR

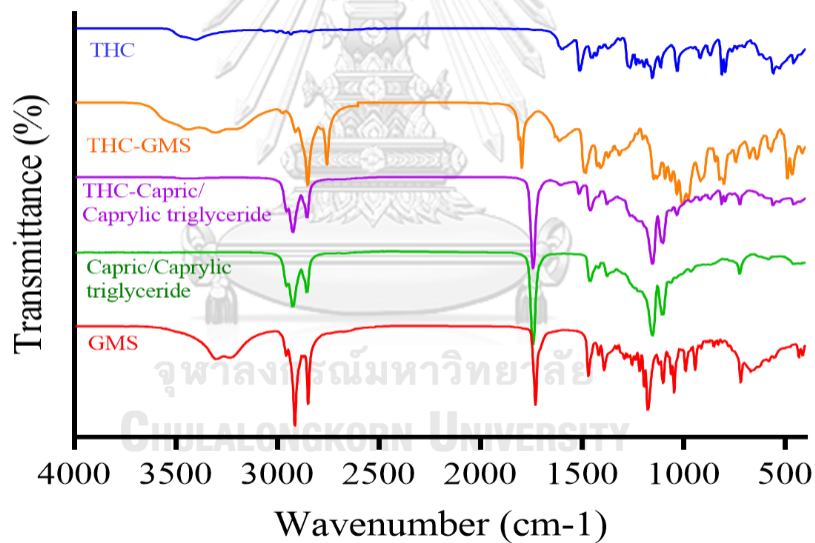
#### 4.1.1. DSC analysis

The drug-excipient compatibility study is a crucial stage in the dosage form development. Here, we used DSC and FT-IR to determine the compatibility of THC and lipids or polymers. Thermal analysis by DSC is a simple tool for detecting physical incompatibilities between components indicated by the absence, appearance or significant shift of melting peaks (shifting range in DSC should be 2-5°C) in the thermogram of drugs or excipients (Rojek & Wesolowski, 2019, Kakkar et al., 2018; El-Kayal et al., 2019). The DSC thermograms of THC, lipids, and binary mixtures are presented in Figure 5a. THC exhibited the presence of sharp endothermic inflection at 103.1 °C with onset and recovery at 89.3 and 112.0 °C, respectively. The melting temperature of THC shown in this study is slightly different from values reported in the literature (92.61 °C) (Trivedi et al., 2020). A slight shift in the melting endotherm of drugs, especially natural products, is expected, which can be associated with impurities in the compound (Pani, Nath, & Acharya, 2011; Verma & Garg, 2005). Additionally, we investigated the thermograms of the binary mixtures of THC and lipids. The THC: capric/caprylic triglyceride mixture showed the endothermic peak of THC at 99.1 °C, indicating that THC is compatible with the liquid lipid. However, the DSC thermogram of THC: GMS mixture revealed a slight shift in the endothermic peak of THC appeared at 93.3 °C that is close to the previously reported melting point of THC. To confirm the possibility of physical incompatibility between THC and GMS, we further analyzed using FT-IR.





(A)



(B)

**Figure 5.** Drug-excipient compatibility: (A) DSC thermograms of THC, GMS, caprylic triglyceride, THC-GMS, and THC- capric/caprylic triglyceride; and (B) IR spectra of pure THC, lipids, and their binary mixtures.

#### 4.1.2. FTIR analysis

The vibrational changes among IR spectra of drug-excipient mixtures can serve as a screening tool to predict their compatibility due to the potential intermolecular interaction between the components (Lima et al., 2013; Pani et al., 2011). To determine the interaction of excipients with the drug, we first analyze the IR spectrum of pure THC. The IR spectrum of THC (Figure 5b) showed a broad absorption band at  $3404\text{ cm}^{-1}$  (-OH group) and an intense band at  $1600\text{ cm}^{-1}$  (carbonyl bond (C=O)). A strong and sharp vibrational band at  $1511\text{ cm}^{-1}$  (aromatic C=C stretching),  $1264\text{ cm}^{-1}$  (enol C-O stretching),  $1031\text{ cm}^{-1}$  (-C-O-CH<sub>3</sub> stretching), absorption bands at  $1451\text{ cm}^{-1}$  (C-H bending of the methyl groups),  $1404\text{ cm}^{-1}$  (O-H bending), and  $1153\text{ cm}^{-1}$  for (C-OH) were observed. The results are consistent with the previous analysis of Trivedi and colleagues (Trivedi et al., 2020).

Furthermore, the individual IR spectra of the lipids and their binary mixtures with THC were scanned and compared to the IR spectrum of pure THC (Figure 5). The characteristic bands of THC in the capric-caprylic acid-THC mixture were observed at  $3411\text{ cm}^{-1}$  (O-H),  $1601\text{ cm}^{-1}$  (C=O),  $1514\text{ cm}^{-1}$  (aromatic C=C),  $1458\text{ cm}^{-1}$  (C-H of methyl groups),  $1418\text{ cm}^{-1}$  (O-H),  $1262\text{ cm}^{-1}$  (C-O of enol),  $1152\text{ cm}^{-1}$  (C-OH), and  $1031\text{ cm}^{-1}$  (-C-O-CH<sub>3</sub>). The characteristic bands of THC in the GMS-THC mixture showed bands at  $3303\text{ cm}^{-1}$  (O-H),  $1600\text{ cm}^{-1}$  (C=O),  $1511\text{ cm}^{-1}$  (aromatic ring),  $1467\text{ cm}^{-1}$  (C-H of methyl groups),  $1391\text{ cm}^{-1}$  (O-H),  $1262\text{ cm}^{-1}$  (C-O of enol),  $1175\text{ cm}^{-1}$  (C-OH), and  $1032\text{ cm}^{-1}$  (-C-O-CH<sub>3</sub>). These results showed that the characteristic bands of THC were well retained in the IR spectra of the binary mixtures without any additional bands and any significant changes in the spectra. Thus, we can deduce that THC is compatible with both lipids used in this study.

## 4.2. Optimization and data analysis by Design-Expert® software

### 4.2.1. Model development for particle size, EE, and DL

RSM is an optimization strategy that enables the prediction of the critical quality attributes of a system by evaluating the significance of the critical material attributes and critical process parameters. Typically, Central Composite Design (CCD) and BBD are the two experimental designs under RSM (Tavares et al., 2021). BBD provides sufficient and statistically analyzed results with a few experimental runs that estimate polynomial equations with first- and second-order coefficients (Bezerra, Santelli, Oliveira, Villar, & Escaleira, 2008). The ranges of the factors were identified from the preliminary one-factor-at-a-time experiments. A total of 15 experiments was performed in a randomized run order to prevent positional bias on the responses (Carr, 2010). The experimental results for the optimization of THC-Ch-NLCs formulation are presented in Table 4. The three responses ranged from 220 to 354 nm for the particle size ( $Y_1$ ), 76.1 to 94.2% for the EE ( $Y_2$ ), and 0.07 to 0.52% for the DL ( $Y_3$ ).

**Table 4.** Box-Behnken experimental design matrix and response values for the optimization of THC-Ch-NLC formulation.

Run	Factors			Responses		
	$X_1$	$X_2$	$X_3$	$Y_1$	$Y_2$	$Y_3$
1	5	0.1	3: 7	268 ± 27.4	83.0 ± 15.0	0.11 ± 0.01
2	15	0.05	3: 7	241 ± 7.7	76.5 ± 0.1	0.22 ± 0.01
3	25	0.1	3: 7	262 ± 11.9	80.6 ± 3.8	0.44 ± 0.02
4	25	0.1	7: 3	331 ± 5.0	79.1 ± 1.8	0.52 ± 0.07
5	15	0.2	7: 3	354 ± 37.6	79.2 ± 0.5	0.34 ± 0.10
6	15	0.1	5: 5	246 ± 10.9	80.0 ± 0.6	0.25 ± 0.02
7	25	0.2	5: 5	282 ± 26.0	82.2 ± 7.0	0.43 ± 0.02
8	5	0.05	5: 5	266 ± 1.6	94.2 ± 0.3	0.1 ± 0.001
9	5	0.1	7: 3	314 ± 10.7	89.4 ± 1.2	0.1 ± 0.01
10	15	0.2	3: 7	226 ± 29.5	84.4 ± 1.4	0.31 ± 0.08
11	5	0.2	5: 5	319 ± 3.8	76.1 ± 2.6	0.07 ± 0.01
12	15	0.1	5: 5	220 ± 7.5	83.7 ± 1.7	0.34 ± 0.05
13	25	0.05	5: 5	265 ± 6.4	76.7 ± 0.5	0.41 ± 0.03
14	15	0.1	5: 5	248 ± 12.9	80.7 ± 0.9	0.24 ± 0.01
15	15	0.05	7: 3	291 ± 3.8	90.6 ± 1.0	0.34 ± 0.04

Multiple linear regression was carried out to determine the RSM models that best describe the relationship among the factors and responses. One-way ANOVA was used to determine the fit of the RSM models. The RSM models were evaluated based on a significant overall model ( $p < 0.05$ ) and non-significant lack-of-fit ( $p > 0.05$ ), reasonable agreement between adjusted  $R^2$  and predicted  $R^2$  (difference is  $< 2$ ), Adeq precision indicating the signal to noise ratio ( $> 4$ ), and significant p-value of each regression coefficient ( $p < 0.05$ ). The model reduction was performed to screen the insignificant terms ( $p > 0.05$ ). The evaluation results indicate the accuracy and

precision of the RSM models, suggesting the closeness between experimental and predicted values.

#### 4.2.2. Response surface analysis

Based on the generated RSM models, the data points of particle size, EE and DL fitted with the quadratic, 2-factor interaction and linear models, respectively (Table 5). The RSM models generated from the optimization are shown in Equations (5) – (7). As shown in Figure 6, the 3D response surface plots the interaction effects of two factors by keeping them constant at their optimal levels while varying the other factor within the experimental range.

$$Y_1 = 244.41 - 7.46X_1 + 14.59X_2 + 40.75X_3 + 19.48X_2X_3 + 33.67X_1^2 + 28.81X_3^2 \quad (5)$$

$$Y_2 = 82.33 - 3.01X_1 - 2.18X_2 + 1.55X_3 + 5.90X_1X_2 - 1.98X_1X_3 - 5.20X_2X_3 \quad (6)$$

$$Y_3 = 0.2813 + 0.1775X_1 + 0.0100X_2 + 0.0275X_3 \quad (7)$$

Equation (5) implies that  $X_2$  and  $X_3$  directly correlate with the size of THC-Ch-NLCs, whereas the THC concentration and solid: liquid lipid ratio shows their quadratic relationships with particle size (Figure 6a-c). The quantity of chitosan and solid: liquid lipid ratio exhibits an interaction effect toward particle size. These effects can be observed with coated nanosystems by dispersing the polymer in the aqueous phase of the nanoparticles. When coated with Ch, the size of nanoparticles increased from 124.56 to 257.5 nm (Silva et al., 2016). The most significant effect was exhibited by  $X_3$ , which may be attributed to the creation of larger particles caused by a higher amount of solid lipids resulting in an increased viscosity of the dispersion.

These findings were established in the comparison tests of cholesterol and cholesteryl stearate (653.12 and 386.7 g/mol, respectively) (Andalib, Varshosaz, Hassanzadeh, & Sadeghi, 2012).

In contrast, increasing the quantity of water-soluble liquid lipid lowered particle size due to a decrease in the formulation's viscosity and surface tension. The amount of the drug also affected the size of the formulation.

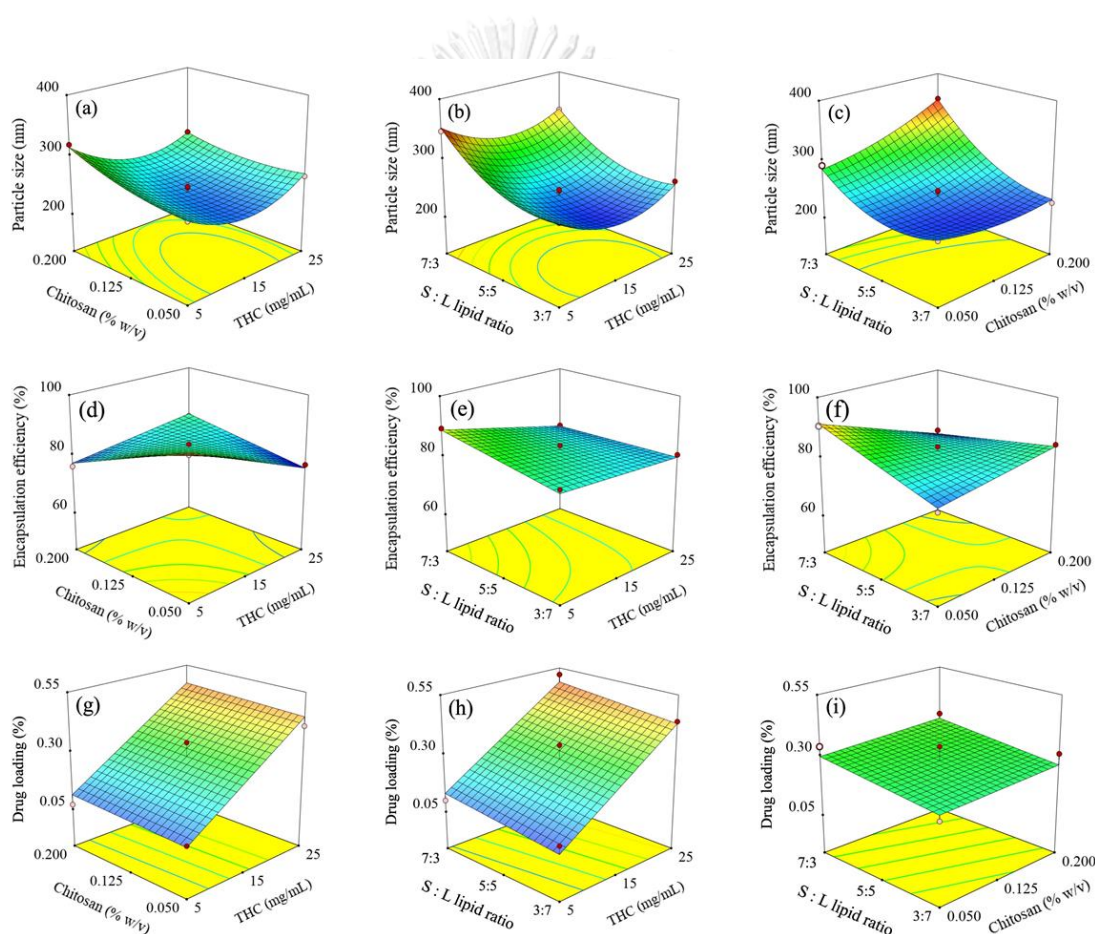


**Figure 6.** Response surface plots showing the effects of THC concentration (X<sub>1</sub>), Ch concentration (X<sub>2</sub>), and S:L lipid ratio (X<sub>3</sub>) on (a-c) particle size (Y<sub>1</sub>), (d-f) EE (Y<sub>2</sub>), and (g-i) DL (Y<sub>3</sub>).

Equation (6) shows that all three factors have interaction effects with each other. These results indicate that the impact of  $X_1$  on EE is affected by the levels of both  $X_2$  and  $X_3$ , resulting in an increase or decrease of EE (Figure 6d-f). The increased distance between fatty acid chains and the voids formed by structural imperfections in the lipid core is essential for including more drugs in the formulation (Asumadu-Mensah, Smith, & Ribeiro 2013). Another study showed that the lipid matrix was more effective when it contained propolis wax and glyceryl behenate than propolis wax alone in entrapment efficiency (Soleimanian, Goli, Varshosaz, & Maestrelli, 2018). Similar to the findings of one study, increasing the drug-to-lipid ratio had a negative correlation with entrapment efficiency (Velmurugan & Selvamuthukumar, 2015). Increased THC concentration resulted in a decrease in encapsulation efficiency. This phenomenon might be caused by the drug being saturated with the polymer and lipid matrix, resulting in the molecule not being encapsulated any longer (Sorasitthyanukarn et al., 2018).

Equation (7) shows the positive effects of  $X_1$ ,  $X_2$ , and  $X_3$  toward DL (Figure 6g-i). An increase in THC concentration, chitosan, and solid: liquid lipid ratio caused an increase in DL. Increasing the amount of  $X_2$  introduced more polymer layers and provided a more substantial barrier preventing the leakage of THC from the lipid core (Sorasitthyanukarn, Muangnoi, Ratnatilaka Na Bhuket, Rojsitthisak, & Rojsitthisak, 2018). Increasing the ratio of the lipids favored an increase of DL, probably due to the retention of THC inside the lipid core resulting in a positive effect on both EE and DL.

**Table 5.** Fit summary of the RSM models

Respond	Source	Sequential p-value	Lack of Fit p-value	Adjusted R <sup>2</sup>	Predicted R <sup>2</sup>	Test of "Adequate precision"
Particle size	Quadratic	0.0042	0.8328	0.9249	0.8278	13.953
DL	Linear	< 0.0001	0.8175	0.9118	0.8735	18.968
EE	2FI	< 0.0001	0.7645	0.9145	0.8404	16.42

#### 4.2.3. Validation of the response surface models

Using the numerical optimization function of Design-Expert®, the optimum formulation of THC-Ch-NLCs was derived from a THC concentration at 16.1 mg/mL, 0.05% chitosan, and 4:6 solid lipid: liquid lipid ratio. The optimized conditions were obtained at desirability (D) of 0.961, which was close to 1.0. The RSM models were validated by preparing the optimized THC-Ch-NLCs and comparing the observed responses with the predicted values obtained from the model equations. The experimental results were similar to the predicted values with % error values of less than 10%, indicating the high predictive ability of the developed RSM models (Table 6).

**Table 6.** Validation of the prediction capability of the RSM models

Optimum conditions	Response	Predicted response	Observed response	% Error
X <sub>1</sub> : 16.1 mg/mL THC,	Y <sub>1</sub> (nm)	225	244 ± 18	8.4
X <sub>2</sub> : 0.05 % (w/v) Ch,	Y <sub>2</sub> (%)	81.1	76.6 ± 0.2	5.3
X <sub>3</sub> : 4:6 solid:liquid lipid ratio	Y <sub>3</sub> (%)	0.28	0.28 ± 0.01	0.7

#### 4.3. Characterization of the optimized formulation

The particle size of THC-Ch-NLCs was found to be 244 ± 18 nm with a distribution index (PDI) of 0.254, indicating a narrow particle size distribution. A



relatively small particle size achieved in the optimum formulation may be related to the presence of an acceptable surfactant concentration, which results in a decrease in surface tension and the formation of particles with small sizes due to the reduction in surface tension (Chaudhary, Garg, Murthy, Rath, & Goyal, 2014). The determined size of THC-Ch-NLCs by dynamic light scattering was further confirmed by the TEM images shown in Figure 7a, which also demonstrated modest aggregation of particles. The zeta potential of THC-Ch-NLCs was  $-17.5 \pm 0.5$  mV. The higher the negative charge, the less likely the nanoparticles would agglomerate together after being stored for an extended period of time. According to the findings of earlier investigations, the lipid nanostructures have a negative charge due to the presence of hydroxyl ions (Witayaudom & Klinkesorn, 2017). It was also revealed that THC-Ch-NLCs had high EE and DL of  $76.6 \pm 0.2\%$  and  $0.28 \pm 0.01\%$ , respectively. A higher EE value implies that the procedure utilized to prepare THC-Ch-NLCs was achieved (Kakkar, Kaur, Kaur, Saini, & Singh, 2018).

DSC is an effective tool for analyzing the melting and crystallization behavior of the lipid materials and drugs in the preparation. The melting behaviors of THC and NLCs formulations are shown in Figure 7b. The thermogram of THC-Ch-NLCs revealed no endothermic peak of THC at  $103.1$  °C, indicating that the drug was successfully encapsulated in the Ch-NLCs in an amorphous state (Al-Shdefat, Yassin, Yassin, Anwer, & Alsarra, 2012; Chandran & Prasanna, 2015).

Figure 7c represents the IR spectra of THC, THC-Ch-NLCs and blank Ch-NLCs to observe the possible interaction of THC when encapsulated in the lipid carrier. The IR spectrum of THC showed absorption bands corresponding to functional groups present in its structure, as discussed in Section 4.1.2. In the spectra

of both THC-Ch-NLCs and blank Ch-NLCs, a broad band of Ch was observed at  $3400\text{ cm}^{-1}$  associated with the  $\text{-NH}_2$  and  $\text{-OH}$  groups in its structure. In addition, bands at  $2887\text{ cm}^{-1}$  ( $\text{-OH}$  stretching),  $1655\text{ cm}^{-1}$  ( $\text{C=O}$  stretching of amide I band), and  $1540\text{-}1600\text{ cm}^{-1}$  ( $\text{N-H}$  bending of amide II band) of Ch were observed on both formulations indicating a successful coating of Ch onto the lipid core (Eid, Ashour, Essa, El Maghraby, & Arafa, 2020; Li, 2008; Sankalia, Mashru, Sankalia, & Sutariya, 2006). Furthermore, the IR spectrum of the formulated THC-Ch-NLCs was compared to those of the blank formulation and pure THC. All major bands of THC overlapped with those of Ch-NLCs, indicating that THC dispersed in the matrix without chemical interaction with the carrier (Keivani Nahr, Ghanbarzadeh, Samadi Kafil, Hamishehkar, & Hoseini, 2019; Sun, Zhao, Ni, & Xia, 2014).

FT-IR analysis of each sample, including Ch, NLCs, THC-NLCs, and THC-Ch-NLCs, was accomplished, and the results are shown in Figure 7c. Pure THC showed characteristic bands, as mentioned in Section 4.1.2. In the IR spectrum of Ch, the bands of O-H stretching, C=O stretching, and N-H bending were at  $2913$ ,  $1735$  and  $1728\text{ cm}^{-1}$ , respectively. A similar pattern between the IR spectra of Ch-NLCs and GMS with no characteristic bands of THC indicates that THC is mainly entrapped in the lipid matrix (Barone et al., 2019).

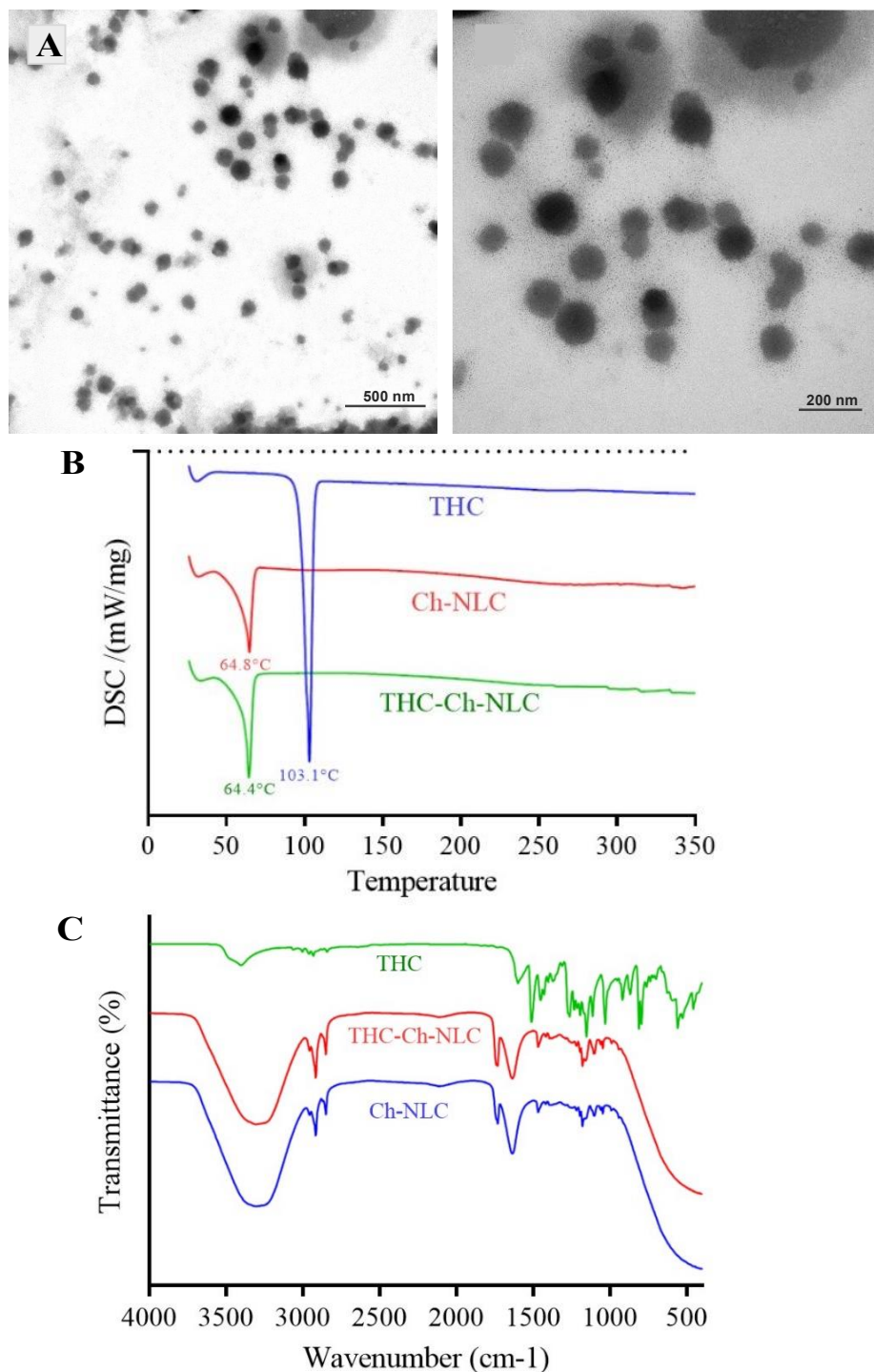


**Figure 7.** Characteristics of the optimized THC-Ch-NLCs: (A) TEM images at 50,000 and 100,000x magnification); (B) DSC thermograms of THC, Ch-NLC and THC-Ch-NLC; and (C) FT-IR spectra of THC, Ch-NLC and THC-Ch-NLC.

#### 4.4. *In vitro* release study of THC from Ch-NLCs and NLCs

Typically, a drug can be integrated into the lipid matrix system of NLCs as dissolved or dispersed form. For drug release from NLCs, solubility of the lipid matrix becomes a critical issue. The release of THC from THC-Ch-NLCs and THC-NLCs in pH 7.4 and 5.5 is shown in Figure 8. The results showed that THC-Ch-NLCs had burst release in the first 12 h, followed by sustained release during the next 24-36 h at pH 7.4 and up to 48 h at pH 5.5.

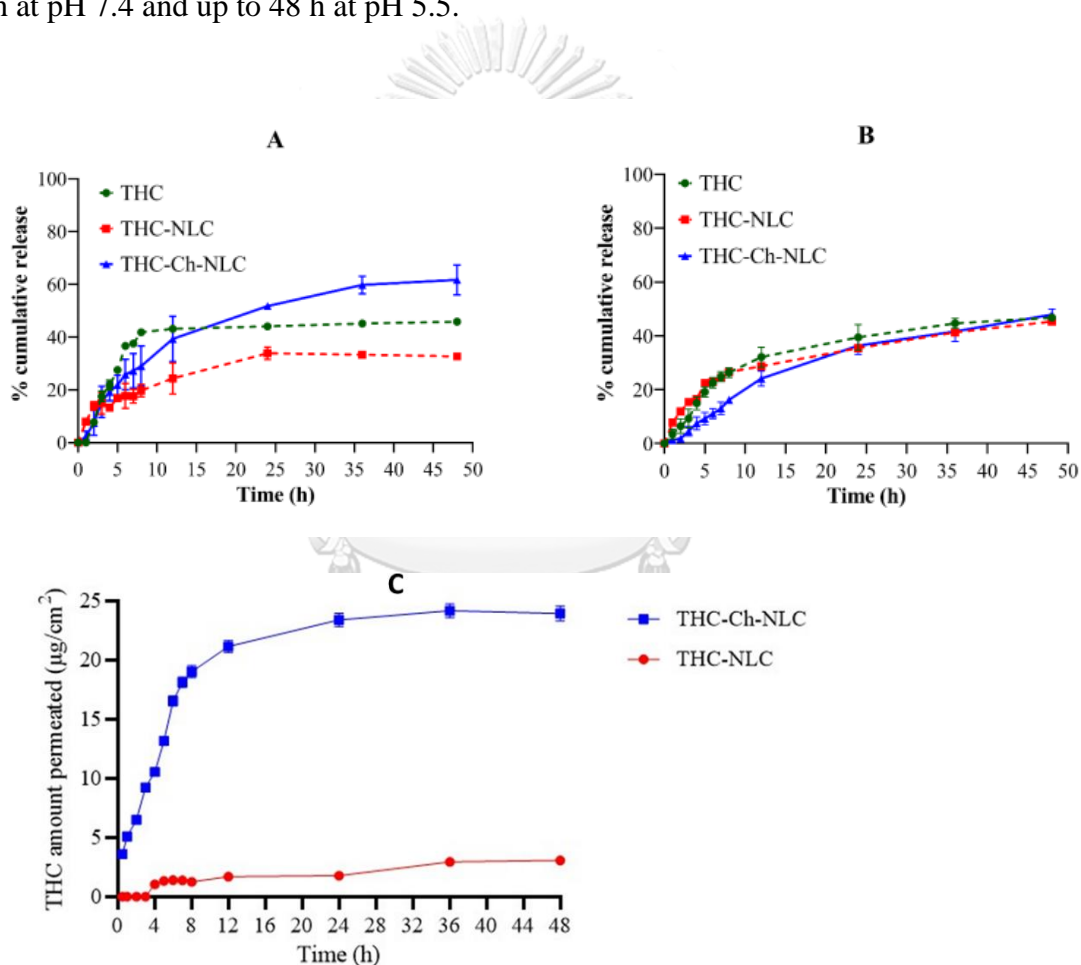


**Figure 8.** Cumulative release of unencapsulated THC and THC from THC-NLCs and THC-Ch-NLCs using the dialysis method at (A) physiological (pH 7.4) and (B) tumor microenvironment (pH 5.5); and (C) permeation profiles of THC from THC-Ch-NLCs and THC-NLCs through Strat-M<sup>®</sup> artificial skin membrane

The physical characteristics of THC-NLC (Size:  $282.8 \pm 1$  nm; EE:  $68.1 \pm 1.4$  %), also showed that with the larger size and lower EE %, limit the release of drug from NLCs.

Furthermore, the release kinetics of THC from the Ch-NLCs and NLCs were determined by fitting the values to different release models. Shown in Table 6 is the summary of the release profile of THC from Ch-NLCs and NLCs in pH 5.5 and 7.4. 30 %v/v ethanol were added in the media used in this study to enhance the solubility of both THC and the lipid in aqueous solution (Barone et al., 2019). THC-Ch-NLCs, in both sink conditions investigated, demonstrated the best match for the Korsmeyer-Peppas release kinetics based on its computed coefficient of determination ( $R^2$ ), the lowest AIC, and the maximum MSC values. The non-linearity of the plots demonstrates that the diffusion pattern did not match with the zero-order kinetic. Korsmeyer and colleagues (Korsmeyer, 1983) reported a straightforward relationship that explained drug release from a polymeric system, and it addresses the possibility of including both drug diffusion and polymer dissolution. Recently, the Peppas–Korsmeyer method has been introduced to lipid nanoparticles, and it has been shown to describe a diffusion-controlled release profile for these particles (Rehman et al., 2015; Shah, Malherbe, Eldridge, Palombo, & Harding, 2014).

**Table 7.** Release kinetics of THC from THC-Ch-NLCs and THC-NLCs in pH 7.4 and 5.5

Model	pH	Sample	Parameter	R <sup>2</sup> <sub>adjusted</sub>	AIC	MSC
Zero order ( $F = k_0 \cdot t$ )	7.4	THC-Ch-NLCs	$k_0 = 1.692$	0.5060	93.4916	0.5386
		THC-NLCs	$k_0 = 0.990$	-0.7439	89.2214	-0.7228
	5.5	THC-Ch-NLCs	$k_0 = 0.992$	0.8814	92.5963	2.0518
		THC-NLCs	$k_0 = 0.929$	0.0116	112.0082	-0.1310
First order ( $F = 100 \cdot e^{-k_1 t}$ )	7.4	THC-Ch-NLCs	$k_1 = 0.031$	0.8269	80.9090	1.5872
		THC-NLCs	$k_1 = 0.014$	-0.3364	86.0276	-0.4567
	5.5	THC-Ch-NLCs	$k_1 = 0.015$	0.9609	76.9867	3.1668
		THC-NLCs	$k_1 = 0.015$	0.3370	106.4185	0.2682
<sup>a</sup> Korsmeyer-Peppas ( $F = k_{KP} \cdot t^n$ )	7.4	THC-Ch-NLCs	$k_{KP} = 20.650,$ $n=0.356$	0.9503	66.8023	2.7627
		THC-NLCs	$k_{KP} = 9.848,$ $n=0.337$	0.9245	52.4024	2.3454
	5.5	THC-Ch-NLCs	$k_{KP} = 3.899,$ $n=0.659$	0.9738	73.0692	3.4465
		THC-NLCs	$k_{KP} = 11.202,$ $n=0.364$	0.9801	58.2000	3.7124
Hixson-Crowell ( $F = 100 \cdot [1 - (1 - k_{HC} \cdot t)^3]$ )	7.4	THC-Ch-NLCs	$k_{HC} = 0.009$	0.7393	85.8238	1.1776
		THC-NLCs	$k_{HC} = 0.004$	-0.4714	87.1823	-0.5529
	5.5	THC-Ch-NLCs	$k_{HC} = 0.004$	0.9412	82.5858	2.7668
		THC-NLCs	$k_{HC} = 0.004$	0.2335	108.4495	0.1232

<sup>a</sup>Best-fit release kinetics model for THC-Ch-NLCs and THC-NLCs, respectively.  $F$  is the fraction (%) of drug released in time,  $t$ ;  $k_0$  is the zero-order release constant;  $k_1$  is the first-order release constant;  $k_{KP}$  is the release constant incorporating structural and geometric characteristics of the drug-dosage form;  $n$  is the diffusional exponent indicating the drug-release mechanism;  $k_{HC}$  is the Hixson-Crowell release constant. The *in-vitro* release data of THC from THC-Ch-NLCs and THC-NLCs in the releasing media

were fitted to Korsmeyer-Peppas for both pH 7.4 and 5.5. This model showed the highest regression coefficient of determination ( $R^2$ ), lowest AIC, and maximal MSC values.

#### **4.5. *In vitro* skin permeation study through Strat-M<sup>®</sup> membrane**

To evaluate the skin permeability of THC from THC-Ch-NLCs, the Strat-M<sup>®</sup> membrane was used to mimic human skin for Franz cell diffusion assay. Figure 8c shows the relative quantity of THC formulation permeated through the artificial membrane. It is noted that we are not able to detect THC permeated for the THC suspension sample up to 48 h. Therefore, we could only determine the impact of Ch-NLCs and NLCs as carriers in the skin permeation study. When compared to THC-NLCs, THC-Ch-NLCs demonstrated a significantly higher permeation through the artificial membrane after 48 h with a flux of 23.9  $\mu\text{g}/\text{cm}^2/\text{h}$ .

It has been shown that NLCs can improve skin permeation through several processes by creating an interaction with skin lipids layers and raising skin moisture levels due to the occlusion of blood flow on skin (Müller, 2002; Wissing, Kayser, & Muller, 2004). Furthermore, the zeta potential of THC-NLC is  $-30 \pm 0.9$  mV, which also affects its permeability as the negatively charged molecule shows less penetrability than the positively charged molecule (Dave et al., 2017). Additionally, positive polymer charges such as Ch may operate as a permeability enhancer by interacting with the biological membrane. Moreover, Ch could open the tight connections of the membrane, facilitating medication distribution to deeper epidermal layers (Taveira et al., 2014; Venancio et al., 2017).

#### 4.6. Cell viability assay

The cytotoxic effects of unencapsulated THC and THC-Ch-NLCs were evaluated in HaCaT cells using the MTT assay (Figure 9). To investigate the effects of THC-Ch-NLC in hyperproliferative HaCaT cells, a psoriasis model was adapted from our previous work (Gomez et al., 2019) by treating the HaCaT cells with TNF- $\alpha$  for 24 h. The induction with TNF- $\alpha$  increased the viable HaCaT cells to 151.27 %, signifying the effective response of the HaCaT cells toward TNF- $\alpha$ . The results of the cell viability of the TNF- $\alpha$ -induced HaCaT cells are shown in Figure 10. In both cases, cell viability was assessed by incubating the HaCaT cells with the Ch-NLCs (as the blank nanoparticles), unencapsulated THC, and THC-Ch-NLCs (as the optimized formulation) at THC concentrations of 1.3 and 6.5  $\mu\text{g/mL}$  for 24 h. Due to the cytotoxicity of the blank to the cell lines further experiment should be done to clarify the effect of THC from THC-NLC and THC-Ch-NLC such as vary the concentration of blank and THC-Ch-NLC between 1.3 – 6.5  $\mu\text{g/mL}$  in the cell cytotoxicity and TNF- $\alpha$  induced HaCaT cells experiment.



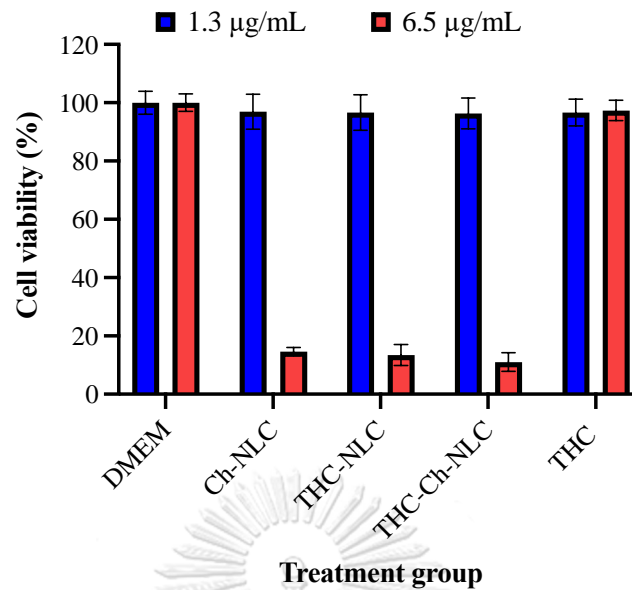


**Figure 9.** The viability of HaCaT cells treated with unencapsulated THC and THC-Ch-NLCs containing different THC concentrations

#### 4.7. Induction of the proliferation of HaCaT cells by TNF- $\alpha$

A comparison of the number of viable cells in the THC-Ch-NLCs and THC-NLCs samples compared to the unstimulated control samples (100 %) revealed that both compounds had anti-psoriatic effects on HaCaT cells (Figure 10). THC-Ch-NLCs and THC-NLCs were compared to free THC at concentrations ranging from 1.3 to 6.5 g/mL. Cell proliferation was raised by 150 percent in the TNF- $\alpha$  (10 ng/ml) group compared to the control group. This indicated that the TNF- $\alpha$  therapy was appropriate for a psoriasis model.

Cell viability was lowered by 5.41 % and 3.78 % in the HaCaT cells induced with TNF- $\alpha$  and treated with THC or THC-Ch-NLCs, respectively, compared to the TNF- $\alpha$  induced cells. Cell viability in the THC-Ch-NLCs and THC-NLCs treated groups was significantly different from that in the TNF- $\alpha$  stimulated cells when the concentration was 6.5  $\mu$ g/mL. Due to the cytotoxicity of blank Ch-NLCs, THC-Ch-

NLCs and THC-NLCs showed considerable suppression of TNF- $\alpha$  induced proliferation of HaCaT cells. However, this may have impacted these findings.

Similar results were obtained from the viabilities of the HaCat cells and TNF- $\alpha$ -induced HaCaT cells. Based on the pairwise comparisons, all treatment groups were not significantly different from the untreated cells (DMEM) at an equivalent THC concentration of 1.3  $\mu\text{g/mL}$ . Further, the viability of cells in THC treatment was not significantly different compared to the untreated cells at 6.5  $\mu\text{g/mL}$ . However, the Ch-NLCs and THC-Ch-NLCs were cytotoxic to the cells at 6.5  $\mu\text{g/mL}$ . Further investigations were conducted to identify which component of the nanocarrier was responsible for these unexpected results. To investigate and possibly eliminate the cytotoxicity potential of chitosan, THC-NLCs were evaluated through the MTT assay. Chitosan has positive amino groups that strongly attract the negatively charged membrane of cells (Qi, Xu, Jiang, Li, & Wang, 2005). Its positive surface charge is responsible for its higher sorption capacity and, therefore, its cytotoxicity. The results showed that even without Ch in the THC-NLC, the nanocarrier was cytotoxic and was not significantly different from the viabilities of the cells toward Ch-NLC and THC-Ch-NLC. It was possible that the combination of the non-ionic surfactant and lipids and the size-dependent cytotoxic effects of NLCs may have increased permeation, resulting in the rupture of the cell membranes (Gomes et al., 2019). The significantly large surface area of the NLCs increased their internalization and could have affected the biological functions of both normal HaCaT and hyperproliferative keratinocyte cells. The optimized formulation, THC-Ch-NLC, significantly showed a higher cytotoxic effect toward the hyperproliferative keratinocyte cells compared to the unencapsulated THC. However, the profound cytotoxic impact of both Ch-NLC and

THC-NLC on the normal HaCaT cells warrants a further investigation of the type and amount of the lipid components and surfactant and their combination in the nano6formulation. This formulation has the potential to be developed as an anti-psoriasis treatment agent or anticancer due to its cytotoxicity properties.

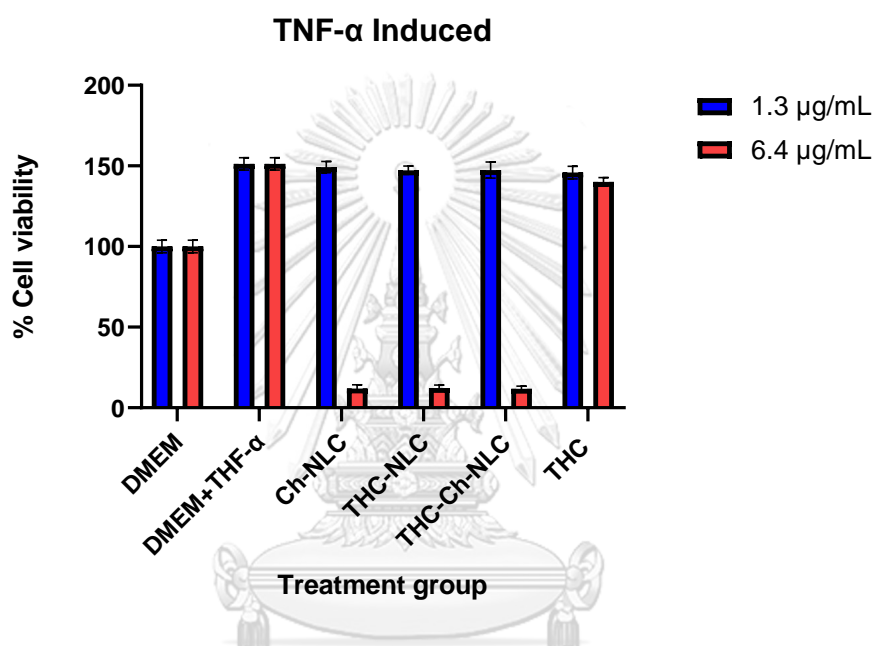


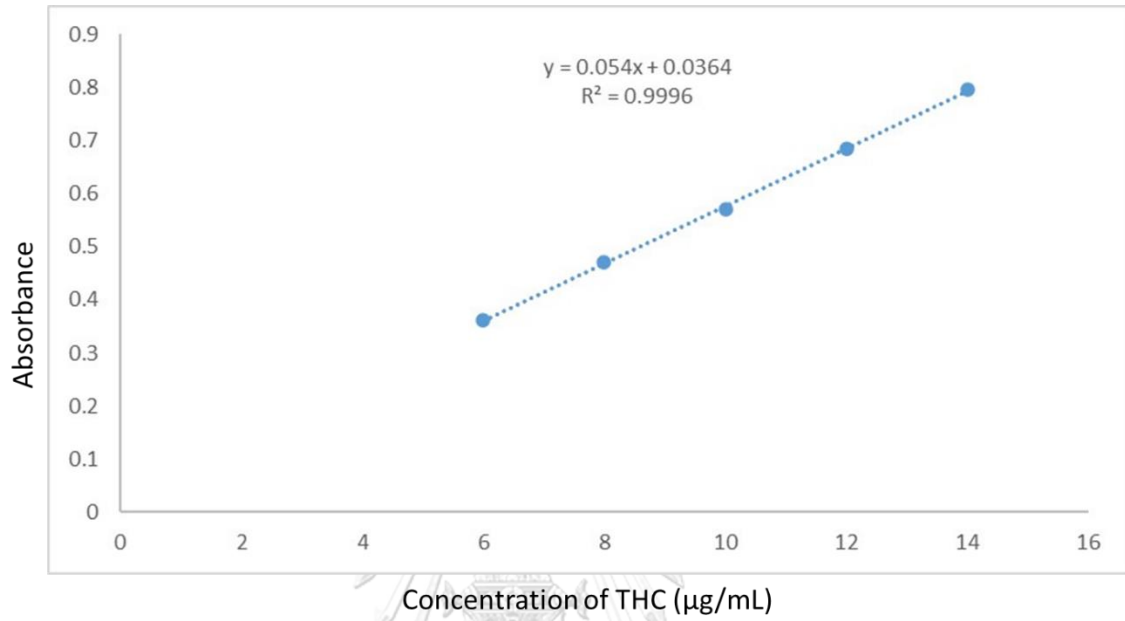
**Figure 10.** The viability of TNF- $\alpha$  induced HaCaT cells treated with unencapsulated THC and THC-Ch-NLCs containing different THC concentrations

## CHAPTER 5 CONCLUSION

To the best of our knowledge, the present study is the first investigation that involves a lipid-based NP formulation of THC for topical delivery to psoriasis. We successfully fabricated and optimized the THC-Ch-NLCs using the Box-Behnken design-based response surface methodology as a tool for analysis. The optimized THC-Ch-NLCs showed sustained THC release in both simulated physiological and tumor microenvironment pH in comparison to THC suspension and THC-NLC. *In vitro* skin permeation study through Strat-M<sup>®</sup> artificial skin membrane showed that THC permeation and retention were higher in Ch-coated NLCs than uncoated NLCs. Furthermore, THC-Ch-NLCs also exhibited cytotoxicity against TNF- $\alpha$ -induced HaCaT cell lines. However, the findings need further investigation to prove that the cytotoxicity was due to the encapsulation of THC in the Ch-NLC since the same cytotoxic effect was also observed in the blank lipid-nanoparticles.

## APPENDIX 1

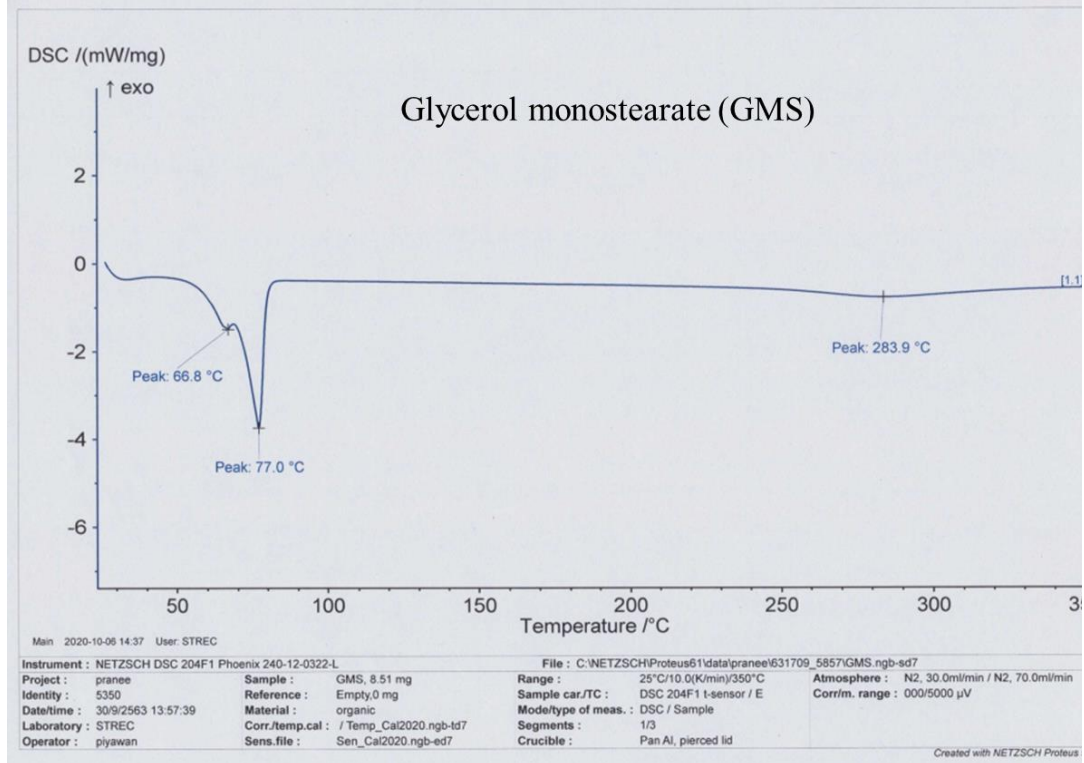
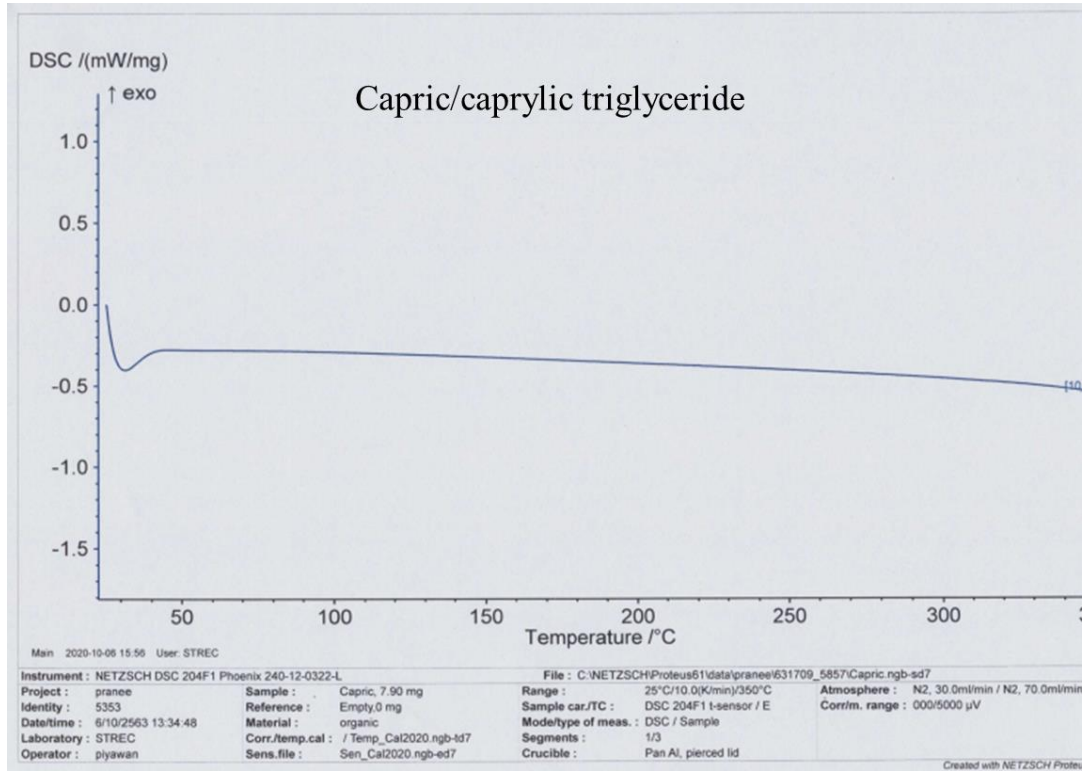
Calibration curve of THC

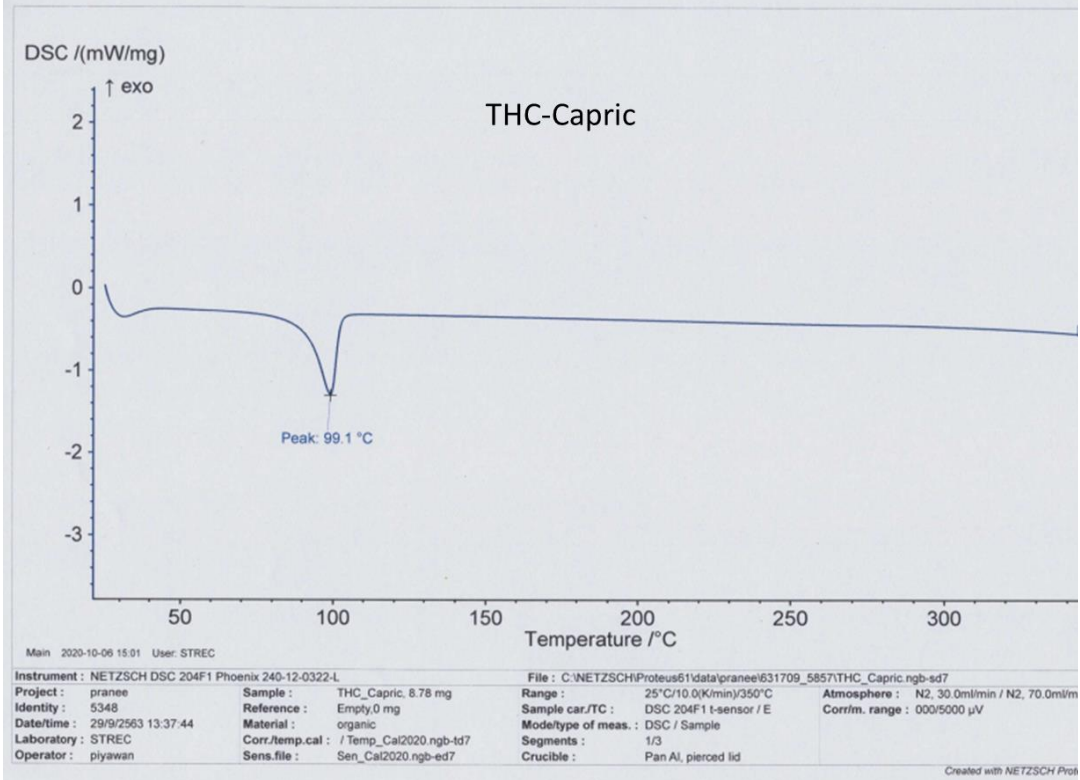
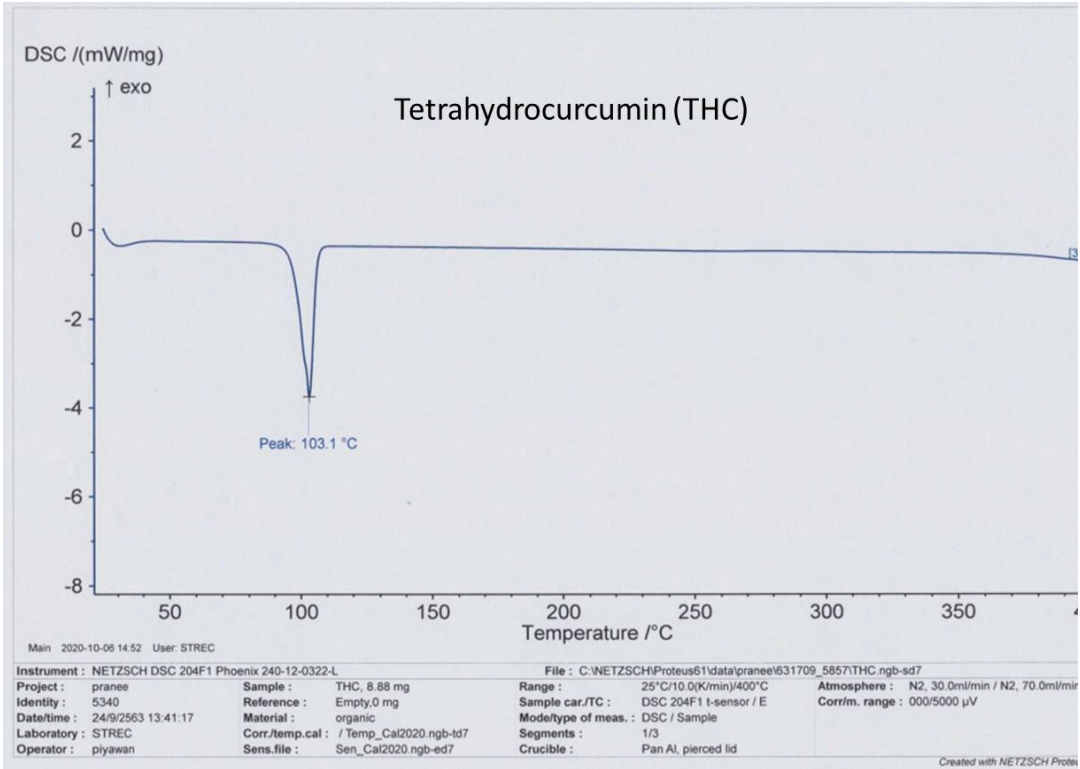


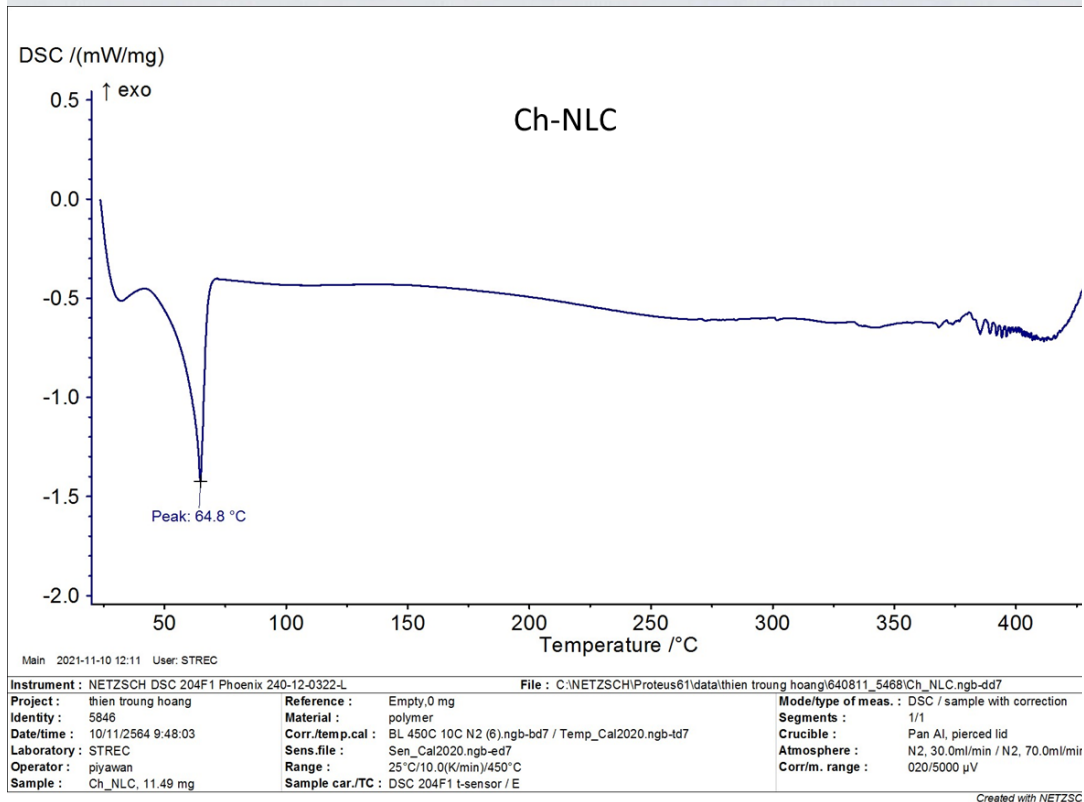
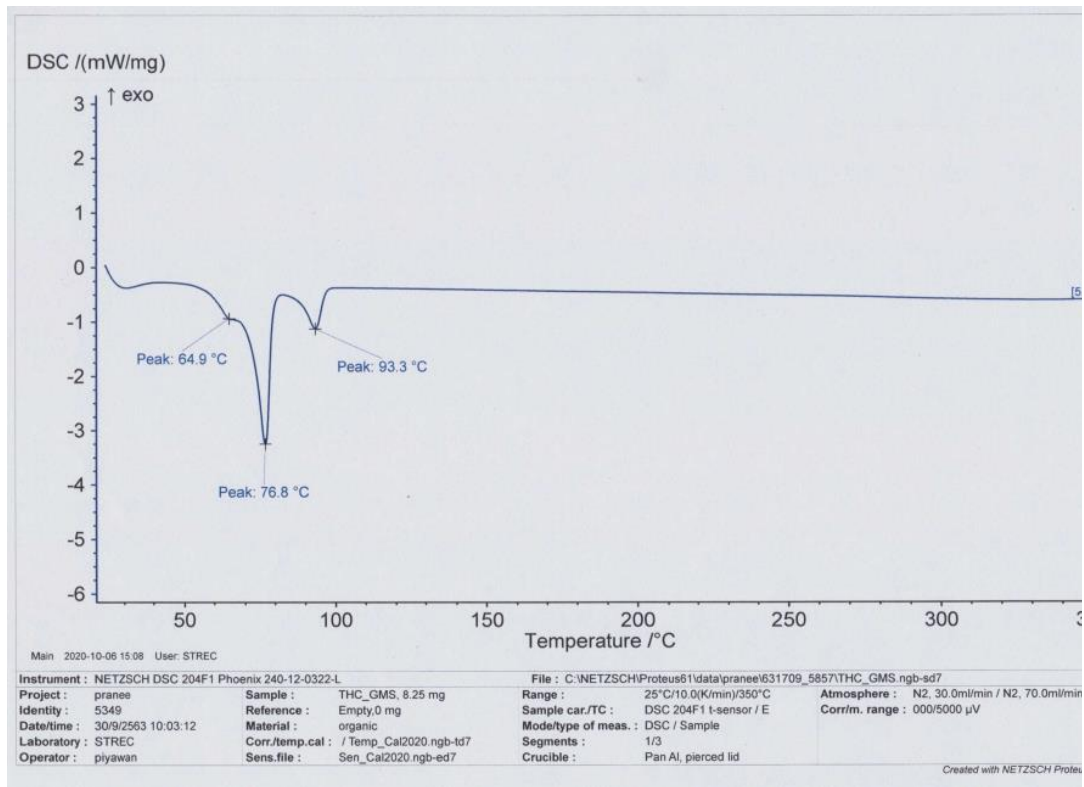
จุฬาลงกรณ์มหาวิทยาลัย  
CHULALONGKORN UNIVERSITY

## APPENDIX 2

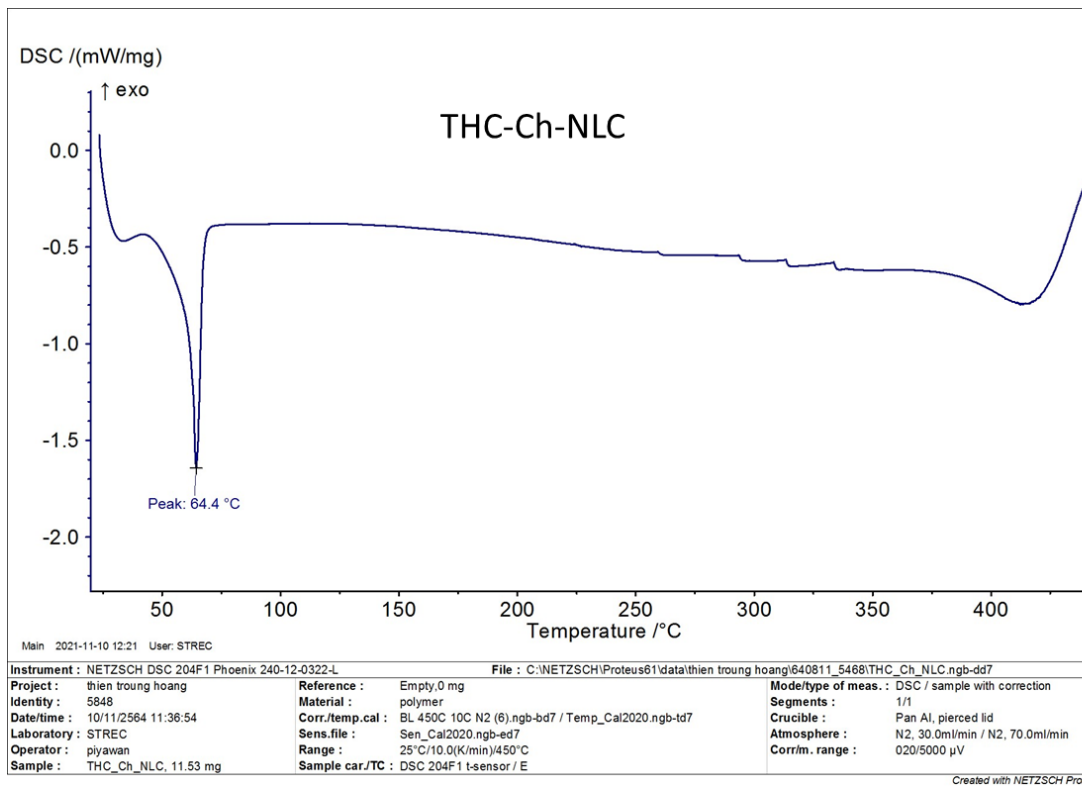
### DSC Thermograms





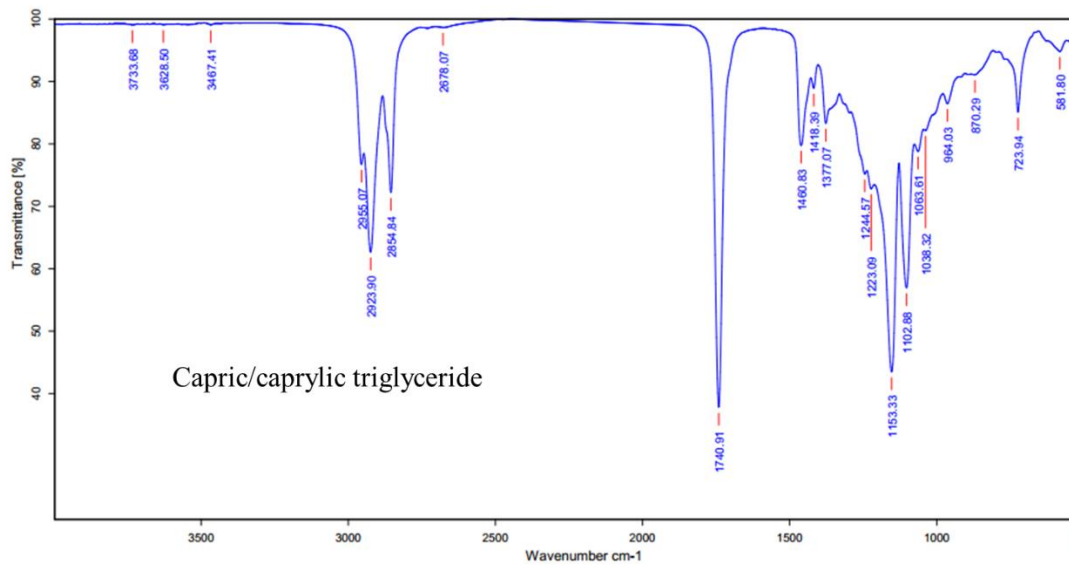
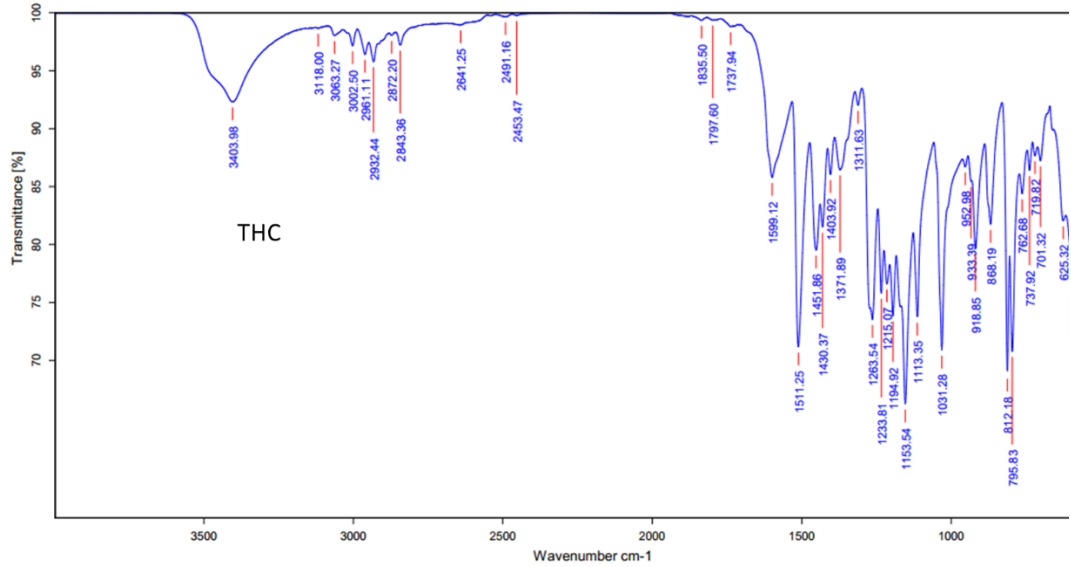


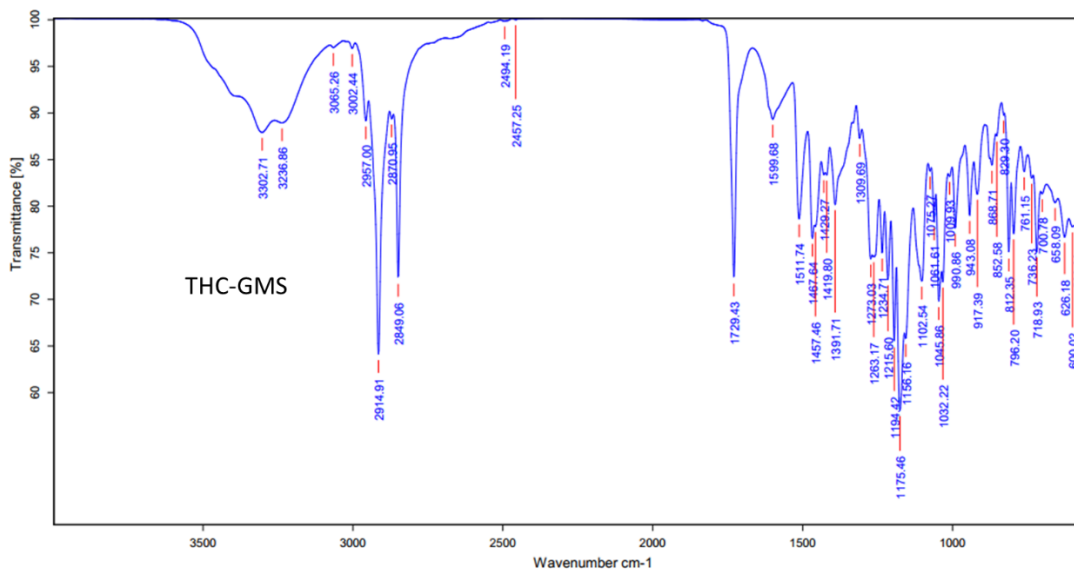
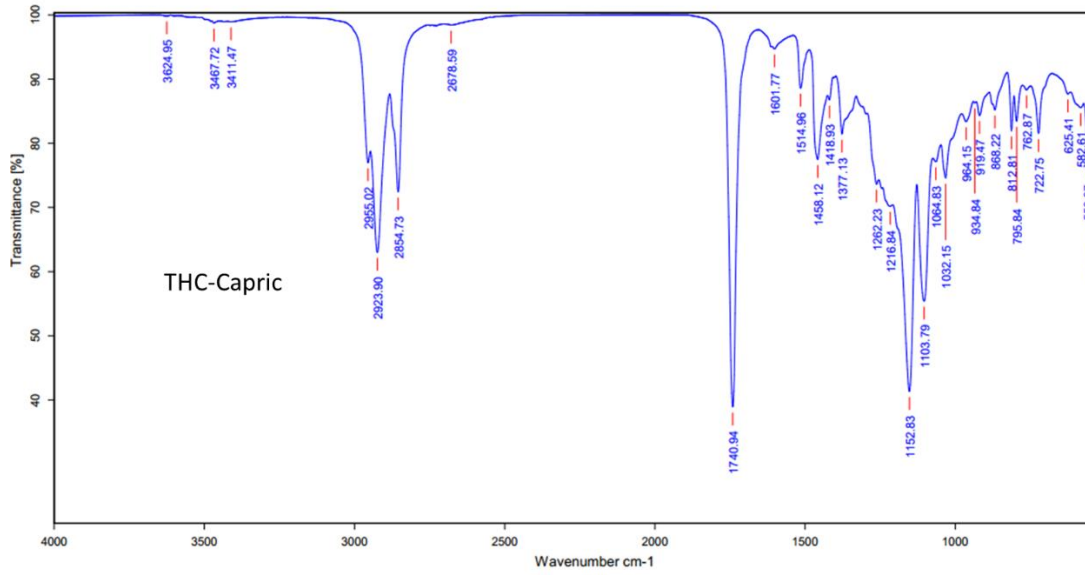
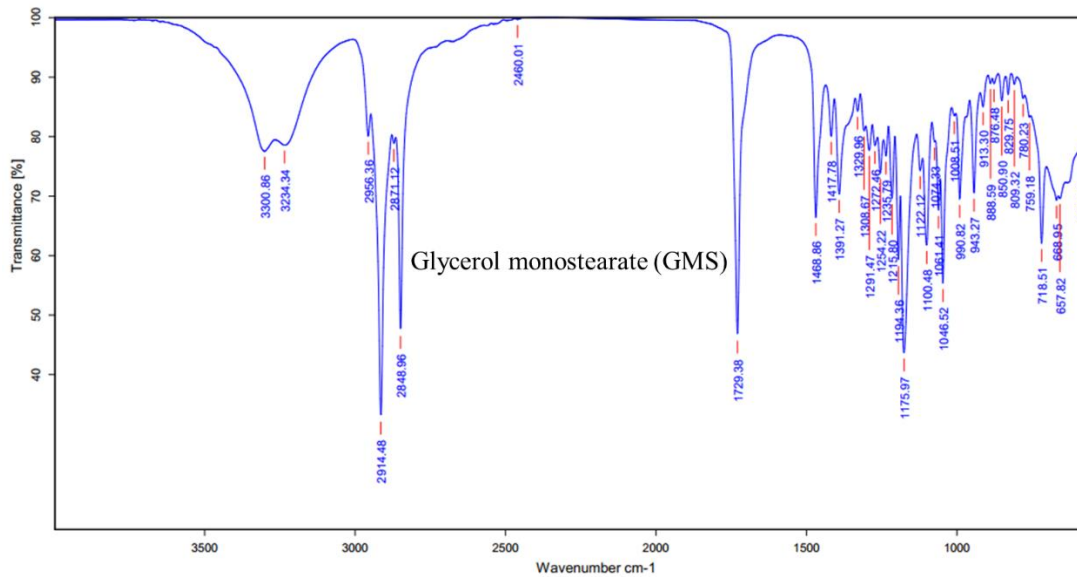


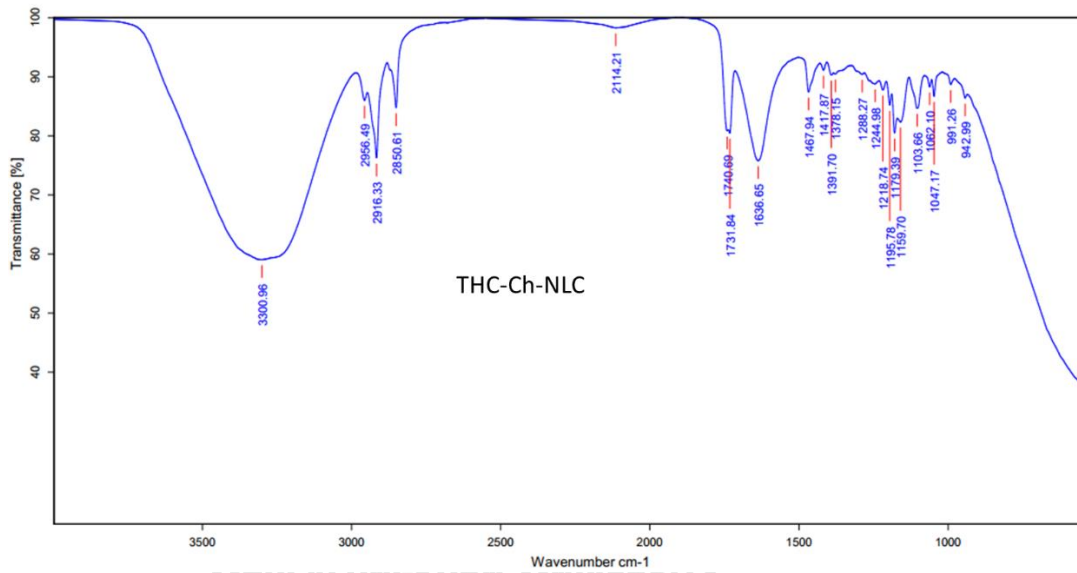
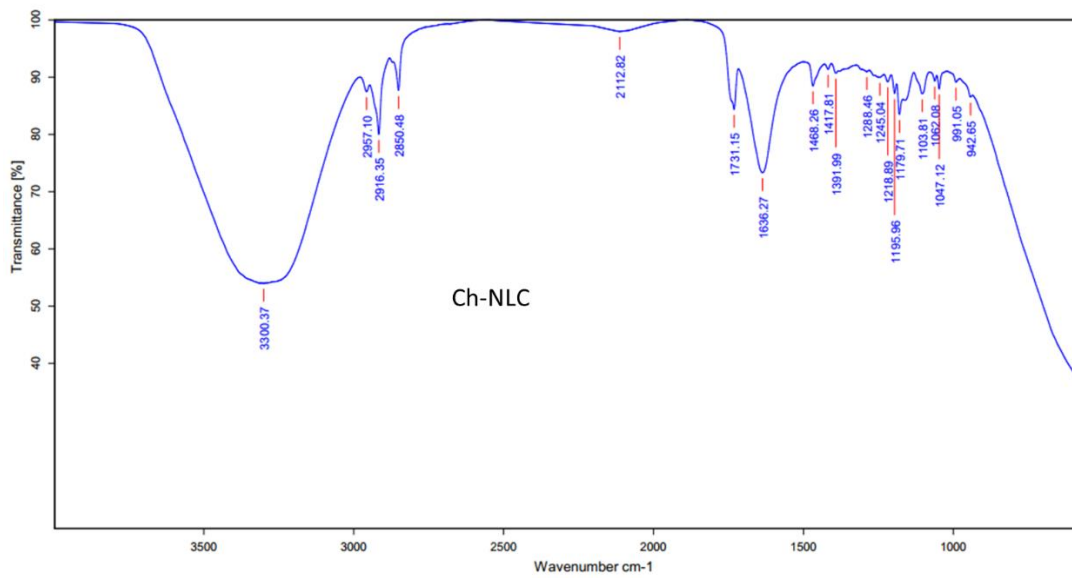


# APPENDIX 3

## FT-IR Spectra







UNIVERSITY

## REFERENCES



จุฬาลงกรณ์มหาวิทยาลัย  
**CHULALONGKORN UNIVERSITY**

- Agnihotri, S. A., Mallikarjuna, N. N., & Aminabhavi, T. M. (2004). Recent advances on chitosan-based micro- and nanoparticles in drug delivery. *Journal of Controlled Release*, 100(1), 5-28.
- Al-Shdefat, R., Yassin, A., Yassin, B., Anwer, M., & Alsarra, I. (2012). Preparation and characterization of biodegradable paclitaxel loaded chitosan microparticles. *Journal of Nanomaterials and Biostructures*, 7(3), 1139-1147.
- Andalib, S., Varshosaz, J., Hassanzadeh, F., & Sadeghi, H. (2012). Optimization of LDL targeted nanostructured lipid carriers of 5-FU by a full factorial design. *Advanced Biomedical Research*, 1, 45.
- Anthony, A. A., Mumuni, A. M., Philip, F. B. (2012). Lipid nanoparticulate drug delivery systems: a revolution in dosage form design and development. *Recent Advances in Novel Drug Carrier Systems*, 107-140.
- Anurag, R., Shalini, S., Sukhbir, K., Ram, S., Bharti, G., Mohammad, F., Sanjula, B., Javed, A. (2015). Nanostructured lipid carrier system for topical delivery of terbinafine hydrochloride. *Cairo University*, 53, 147–159.
- Asumadu, A., Smith, W., Ribeiro, S. (2013). Solid lipid dispersions: potential delivery system for functional ingredients in foods. *Journal of Food Science*, 78(7), 1000-1008.
- Bai, F., Zheng, W., Dong, Y., Wang, J., Garstka, M. A., Li, R., An, J., & Ma, H. (2017). Serum levels of adipokines and cytokines in psoriasis patients: a systematic review and meta-analysis. *Oncotarget*, 9(1), 1266–1278.
- Baliwag, J., Barnes, H., Johnston, A. (2015). Cytokines in psoriasis. *Cytokine*, 73, 343–350.
- Barone, A., Mendes, M., Cabral, C., Mare, R., Paolino, D., & Vitorino, C. (2019). Hybrid nanostructured films for topical administration of simvastatin as coadjuvant treatment of melanoma. *Journal of Pharmaceutical Sciences*, 108(10), 3396–3407.

- Bartosova, L., & Bajgar, J. (2012). Transdermal drug delivery in vitro using diffusion cells. *Current Medicinal Chemistry*, 19(27), 4671–4677.
- Barzegar-Jalali, M., Adibkia, K., Valizadeh, H., Shadbad, M. R., Nokhodchi, A., Omid, Y., Mohammadi, G., Nezhadi, S. H., & Hasan, M. (2008). Kinetic analysis of drug release from nanoparticles. *Journal of Pharmacy & Pharmaceutical Sciences*, 11(1), 167–177.
- Beck, R., Guterres, S., Pohlmann, A. (2011). Nanocosmetics and nanomedicines: new approaches for skin care. *Nanocosmetics and Nanomedicines*. Springer. 101-122.
- Beloqui, A., Solinís, M. Á., Delgado, A., Evora, C., Isla, A., & Rodríguez-Gascón, A. (2014). Fate of nanostructured lipid carriers (NLCs) following the oral route: design, pharmacokinetics and biodistribution. *Journal of Microencapsulation*, 31(1), 1-8.
- Beloqui, A., Solinís, M. Á., Rodríguez-Gascón, A., Almeida, A. J., & Prétat, V. (2016). Nanostructured lipid carriers: Promising drug delivery systems for future clinics. *Nanomedicine: Nanotechnology, Biology, and Medicine*, 12(1), 143–161.
- Bezerra, M. A., Santelli, R. E., Oliveira, E. P., Villar, L. S., & Escaleira, L. A. (2008). Response surface methodology (RSM) as a tool for optimization in analytical chemistry. *Talanta*, 76(5), 965-977.
- Bharti, G., Mohammad, F., Saba, K., Asgar, A., Sanjula, B., Javed, A. (2015). Nanostructured lipid carrier system for topical delivery of terbinafine hydrochloride. *Bulletin of Faculty of Pharmacy, Cairo University*, 53, 147–159.
- Bolognia, L., Jorizzo, L., Schaffer, V. (2012). *Dermatology*. 3rd ed. St. Louis: Elsevier Health Sciences; [chapter 124].
- Boonyasirisri, P., Nimmannit, U., Rojsitthisak, P., Bhunchu, S., Rojsitthisak, P. (2015). Optimization of curcuminoid-loaded PLGA nanoparticles using Box-Behnken statistical design. *Journal of Nano Research*, 33, 60-71,

- Bright, J. (2007). Curcumin and autoimmune disease. *Advances in Experimental Medicine and Biology*, 595, 425–451.
- Carr, B. T. (2014). Statistical design of experiments in the 21st century and implications for consumer product testing. *In Woodhead Publishing Series in Food Science, Technology and Nutrition*, 2010, 427-469.
- Coppi, G., & Iannuccelli, V. (2009). Alginate/chitosan microparticles for tamoxifen delivery to the lymphatic system. *International Journal of Pharmaceutics*, 367(1-2), 127–132.
- Chandran, I., & Prasanna, P. (2015). Drug-Excipient interaction studies of loperamide loaded in polysorbate 80 liposomes. *Oriental Journal of Chemistry*, 31(4), 2201-2206.
- Chaudhary, S., Garg, T., Murthy, R. S., Rath, G., & Goyal, A. K. (2014). Recent approaches of lipid-based delivery system for lymphatic targeting via oral route. *Journal of Drug Targeting*, 22(10), 871-882.
- Chellat, F., Merhi, Y., Moreau, A., & Yahia, L. (2005). Therapeutic potential of nanoparticulate systems for macrophage targeting. *Biomaterials*, 26(35), 7260–7275.
- Chen, C. C., Tsai, T. H., Huang, Z. R., & Fang, J. Y. (2010). Effects of lipophilic emulsifiers on the oral administration of lovastatin from nanostructured lipid carriers: physicochemical characterization and pharmacokinetics. *European Journal of Pharmaceutics and Biopharmaceutics*, 74(3), 474–482.
- Chinsriwongkul, A., Chareanputtakhun, P., Ngawhirunpat, T., Rojanarata, T., Sila-on, W., Ruktanonchai, U., & Opanasopit, P. (2012). Nanostructured lipid carriers (NLC) for parenteral delivery of an anticancer drug. *AAPS PharmSciTech*, 13(1), 150–158.
- Das, R. K., Kasoju, N., & Bora, U. (2010). Encapsulation of curcumin in alginate-chitosan-pluronic composite nanoparticles for delivery to cancer cells. *Nanomedicine: Nanotechnology, Biology, and Medicine*, 6(1), 153–160.



- Dave, K., & Krishna Venuganti, V. V. (2017). Dendritic polymers for dermal drug delivery. *Therapeutic Delivery*, 8(12), 1077–1096.
- Duan, J., Mansour, H. M., Zhang, Y., Deng, X., Chen, Y., Wang, J., Pan, Y., & Zhao, J. (2012). Reversion of multidrug resistance by co-encapsulation of doxorubicin and curcumin in chitosan/poly (butyl cyanoacrylate) nanoparticles. *International Journal of Pharmaceutics*, 426(1-2), 193–201.
- Eid, R. K., Ashour, D. S., Essa, E. A., El Maghraby, G. M., & Arafa, M. F. (2020). Chitosan coated nanostructured lipid carriers for enhanced in vivo efficacy of albendazole against *Trichinella spiralis*. *Carbohydrate Polymers*, 232, 115826.
- El-Kayal, M., Nasr, M., Elkheshen, S., & Mortada, N. (2019). Colloidal (-)-epigallocatechin-3-gallate vesicular systems for prevention and treatment of skin cancer: A comprehensive experimental study with preclinical investigation. *European Journal of Pharmaceutical Sciences*, 137, 104972.
- Fonte, P., Nogueira, T., Gehm, C., Ferreira, D., & Sarmiento, B. (2011). Chitosan-coated solid lipid nanoparticles enhance the oral absorption of insulin. *Drug Delivery and Translational Research*, 1(4), 299–308.
- Garcia-Fuentes, M., Torres, D., & Alonso, M. J. (2005). New surface-modified lipid nanoparticles as delivery vehicles for salmon calcitonin. *International Journal of Pharmaceutics*, 296(1-2), 122–132.
- George, M., & Abraham, E. (2006). Polyionic hydrocolloids for the intestinal delivery of protein drugs: alginate and chitosan—a review. *Journal of Controlled Release*, 114(1), 1-14.
- Global Report on Psoriasis (2016). World Health Organization: Geneva, Switzerland, 2016.
- Gomes, G., Sola, M. R., Rochetti, A. L., Fukumasu, H., Vicente, A. A., & Pinho, S. C. (2019).  $\beta$ -carotene and  $\alpha$ -tocopherol coencapsulated in nanostructured lipid carriers of murumuru (*Astrocaryum murumuru*) butter produced by phase inversion temperature method: characterisation, dynamic in vitro digestion and cell viability study. *Journal of Microencapsulation*, 36(1), 43–52.

- Gomez, C., Muangnoi, C., Sorasitthyanukarn, F. N., Wongpiyabovorn, J., Rojsitthisak, P., & Rojsitthisak, P. (2019). Synergistic effects of photo-irradiation and curcumin-chitosan/alginate nanoparticles on tumor necrosis factor-alpha-induced psoriasis-like proliferation of keratinocytes. *Molecules (Basel, Switzerland)*, 24(7), 1388.
- Hawkes, J. E., Chan, T. C., & Krueger, J. G. (2017). Psoriasis pathogenesis and the development of novel targeted immune therapies. *The Journal of Allergy and Clinical Immunology*, 140(3), 645–653.
- Heath, D. D., Pruitt, M. A., Brenner, D. E., Begum, A. N., Frautschy, S. A., & Rock, C. L. (2005). Tetrahydrocurcumin in plasma and urine: quantitation by high performance liquid chromatography. *Journal of Chromatography. B, Analytical Technologies in the Biomedical and Life Sciences*, 824(1-2), 206–212.
- Higgins, E. (2017). Psoriasis. *Medicine*, 45(6), 368–378.
- Jana, P., Aiman, H., Rainer, H. & Müller, H. (2009). Lipid nanoparticles (SLN, NLC) in cosmetic and pharmaceutical dermal products. *International Journal of Pharmaceutics*, 366, 170–184.
- Jayakumar, R., Menon, D., Manzoor, K., Nair, S. V., & Tamura, H. (2010). Biomedical applications of chitin and chitosan based nanomaterials—A short review. *Carbohydrate Polymers*, 82 (2), 227-232.
- Jia, L. J., Zhang, D. R., Li, Z. Y., Feng, F. F., Wang, Y. C., Dai, W. T., Duan, C. X., & Zhang, Q. (2010). Preparation and characterization of silybin-loaded nanostructured lipid carriers. *Drug Delivery*, 17(1), 11–18.
- Jinhua, D., (2012). Reversion of multidrug resistance by co-encapsulation of doxorubicin and curcumin in chitosan/poly (butyl cyanoacrylate) nanoparticles. *International Journal of Pharmaceutics*, 426, 193–201.
- Kakkar, V., Kaur, I. P., Kaur, A. P., Saini, K., & Singh, K. K. (2018). Topical delivery of tetrahydrocurcumin lipid nanoparticles effectively inhibits skin

- inflammation: in vitro and in vivo study. *Drug Development and Industrial Pharmacy*, 44(10), 1701-1712.
- Kamble, S., & Vaidya, K. (2012). Solid lipid nanoparticles and nanostructured lipid carriers – an overview. *International Journal of Pharmaceutical, Chemical and Biological Sciences*, 2, 681–691.
- Keivani Nahr, F., Ghanbarzadeh, B., Samadi Kafil, H., Hamishehkar, H., & Hoseini, M. (2019). The colloidal and release properties of cardamom oil encapsulated nanostructured lipid carrier. *Journal of Dispersion Science and Technology*, 42(1), 1-9.
- Kelly, J. B., 3rd, Foley, P., & Strober, B. E. (2015). Current and future oral systemic therapies for psoriasis. *Dermatologic Clinics*, 33(1), 91–109.
- Kim, M. Y., Lim, Y. Y., Kim, H. M., Park, Y. M., Kang, H., & Kim, B. J. (2015). Synergistic inhibition of tumor necrosis factor-alpha-stimulated pro-inflammatory cytokine expression in HaCaT cells by a combination of rapamycin and mycophenolic acid. *Annals of dermatology*, 27(1), 32–39.
- Korsmeyer, R. W., Gurny, R., Doelker, E., Buri, P., & Peppas, N. A. . (1983). Mechanisms of potassium chloride release from compressed, hydrophilic, polymeric matrices- effect of entrapped air. *Journal of Pharmaceutical Sciences*, 72(10), 1189–1191.
- Krambeck, K., Silva, V., Silva, R., Fernandes, C., Cagide, F., Borges, F., . . . Amaral, M. H. (2021). Design and characterization of nanostructured lipid carriers (NLC) and nanostructured lipid carrier-based hydrogels containing *Passiflora edulis* seeds oil. *International Journal of Pharmaceutics*, 600, 120444.
- Kumar, K., Sasikanth, K., Sabareesh, M., & Dorababu, N. (2011). Formulation and evaluation of diacerein cream. *Asian Journal of Pharmaceutical and Clinical Research*, 4, 93-98.
- Kushwaha, A. K., Vuddanda, P. R., Karunanidhi, P., Singh, S. K., & Singh, S. (2013). Development and evaluation of solid lipid nanoparticles of raloxifene

- hydrochloride for enhanced bioavailability. *BioMed research international*, 2013, 584549.
- Khoushab, F., & Yamabhai, M. (2010). Chitin research revisited. *Marine Drugs*, 8(7), 1988–2012.
- Lee, E. H., Lim, S. J., & Lee, M. K. (2019). Chitosan-coated liposomes to stabilize and enhance transdermal delivery of indocyanine green for photodynamic therapy of melanoma. *Carbohydrate Polymers*, 224, 115143.
- Le-Jiao, J. (2010). Preparation and characterization of silybin-loaded nanostructured lipid carriers. *Drug Delivery*, 17(1): 11–18.
- Lertsutthiwong, P., & Rojsitthisak, P. (2011). Chitosan-alginate nanocapsules for encapsulation of turmeric oil. *Die Pharmazie*, 66(12), 911–915.
- Leticia, M., (2019). The role of chitosan as coating material for nanostructured lipid carriers for skin delivery of fucoxanthin. *International Journal of Pharmaceutics*, 567, 118487.
- Li, F., Weng, Y., Wang, L., He, H., Yang, J., & Tang, X. (2010). The efficacy and safety of bufadienolides-loaded nanostructured lipid carriers. *International Journal of Pharmaceutics*, 393(1-2), 203–211.
- Li, P., Dai, Y. N., Zhang, J. P., Wang, A. Q., & Wei, Q. (2008). Chitosan-alginate nanoparticles as a novel drug delivery system for nifedipine. *International Journal of Biomedical Science*, 4(3), 221–228.
- Lima, N. G. P. B., Lima, I. P. B., Barros, D. M. C., Oliveira, T. S., Raffin, F. N., de Lima e Moura, T. F. A., .Aragão, C. F. S. (2013). Compatibility studies of trioxsalen with excipients by DSC, DTA, and FTIR. *Journal of Thermal Analysis and Calorimetry*, 115(3), 2311-2318.
- Lin, J., Cai, Q., Tang, Y., Xu, Y., Wang, Q., Li, T., Lin, D. (2018). PEGylated lipid bilayer coated mesoporous silica nanoparticles for co-delivery of paclitaxel and curcumin: Design, characterization and its cytotoxic effect. *International Journal of Pharmaceutics*, 536(1), 272-282.

- Long, Y., Dean, K., & Li, L. (2006). Polymer blends and composites from renewable resources. *Progress in Polymer Science*, 31(6), 576-602.
- Luesakul, U., Puthong, S., Sansanaphongpricha, K., & Muangsin, N. (2020). Quaternized chitosan-coated nanoemulsions: A novel platform for improving the stability, anti-inflammatory, anti-cancer and transdermal properties of Plai extract. *Carbohydrate Polymers*, 230, 115625.
- Malgarim Cordenonsi, L., Faccendini, A., Catanzaro, M., Bonferoni, M. C., Rossi, S., Malavasi, L., Platchek Raffin, R., Scherman Schapoval, E. E., Lanni, C., Sandri, G., & Ferrari, F. (2019). The role of chitosan as coating material for nanostructured lipid carriers for skin delivery of fucoxanthin. *International Journal of Pharmaceutics*, 567, 118487.
- Martínez, M., Rodríguez, G., Gonzalez, I., Hernández, M., Corma, A., Bermejo, M., Merino, V., & Gonzalez, M. (2018). Ionic hydrogel based on chitosan cross-linked with 6-phosphogluconic trisodium salt as a drug delivery system. *Biomacromolecules*, 19(4), 1294-1304.
- Mbah, C. J., Uzor, P. F., & Omeje, E. O. (2011). Perspective on transdermal drug delivery. *Journal of Chemical and Pharmaceutical Research*, 3(3):680-700.
- Meng, S., Lin, Z., Wang, Y., Wang, Z., Li, P., & Zheng, Y. (2018). Psoriasis therapy by Chinese medicine and modern agents. *Chinese medicine*, 13, 16.
- Montagna, W., & Parakkal, F. (1974). *The structure and function of skin*. 3rd ed. Academic Press New York and London.
- Montenegro, L., Lai, F., Offera, A., Sarpietro, G., Micicche, L., & Maccioni, M. (2016). From nanoemulsions to nanostructured lipid carriers: a relevant development in dermal delivery of drugs and cosmetics. *Journal of Drug Delivery Science and Technology*, 32, 100–112.
- Motiei, M., Kashanian, S., Lucia, A., & Khazaei, M. (2017). Intrinsic parameters for the synthesis and tuned properties of amphiphilic chitosan drug delivery nanocarriers. *Journal of Controlled Release*, 260, 213-225.

- Muhammad, M., Gertru, C., & Gabriel, J. (2010). A randomized, double-blind, placebo-controlled, comparative study. *Household Pers Care Today*, 3,44–46.
- Müller, R. H., Radtke, M., & Wissing, S. A. (2002). Nanostructured lipid matrices for improved microencapsulation of drugs. *International Journal of Pharmaceutics*, 242(1-2), 121–128.
- Nakamura, Y., Ohto, Y., Murakami, A., Osawa, T., & Ohigashi, H. (1998). Inhibitory effects of curcumin and tetrahydrocurcuminoids on the tumor promoter-induced reactive oxygen species generation in leukocytes in vitro and in vivo. *Japanese Journal of Cancer Research: Gann*, 89(4), 361–370.
- Natarajan, J., Karri, R., & Anindita, D. (2017). Nanostructured lipid carrier (NLC): a promising drug delivery system. *Global Journal of Nnomedicine*, 1, 20-25
- National center for biotechnology information (2021). PubChem Patent Summary for DE-69232914-T2. Retrieved December 27, 2021.
- Nedoszytko, B., Sokołowska-Wojdyło, M., Ruckemann-Dziurdzińska, K., Roszkiewicz, J., & Nowicki, R. J. (2014). Chemokines and cytokines network in the pathogenesis of the inflammatory skin diseases: atopic dermatitis, psoriasis and skin mastocytosis. *Postepy Dermatologii I Alergologii*, 31(2), 84–91.
- Okonogi, S., & Riangjanapatee, P. (2015). Physicochemical characterization of lycopene-loaded nanostructured lipid carrier formulations for topical administration. *International Journal of Pharmaceutics*, 478(2), 726–735.
- Osawa, T., Sugiyama, Y., Inayoshi, M., & Kawakishi, S. (1995). Antioxidative activity of tetrahydrocurcuminoids. *Bioscience, Biotechnology, and Biochemistry*, 59(9), 1609–1612.
- Pan, M. H., Huang, T. M., & Lin, J. K. (1999). Biotransformation of curcumin through reduction and glucuronidation in mice. *Drug Metabolism and Disposition*, 27(4), 486–494.

- Pani, D. N., Nath, L., & Acharya, S. (2011). Application of DSC, IST, and FTIR study in the compatibility testing of nateglinide with different pharmaceutical excipients. *Journal of Thermal Analysis and Calorimetry*, 108(1), 219–226.
- Pardeike, J., Weber, S., Zarfl, H. P., Pagitz, M., & Zimmer, A. (2016). Itraconazole-loaded nanostructured lipid carriers (NLC) for pulmonary treatment of aspergillosis in falcons. *European Journal of Pharmaceutics and Biopharmaceutics*, 108, 269–276.
- Park, S. J., Garcia, C. V., Shin, G. H., & Kim, J. T. (2017). Development of nanostructured lipid carriers for the encapsulation and controlled release of vitamin D3. *Food Chemistry*, 225, 213–219.
- Parveen, S., & Sahoo, K. (2008). Polymeric nanoparticles for cancer therapy. *Journal of Drug Targeting*, 16 (2), 108-123.
- Plyduang, T., Lomlim, L., Yuenyongsawad, S., & Wiwattanapatapee, R. (2014). Carboxymethylcellulose-tetrahydrocurcumin conjugates for colon-specific delivery of a novel anti-cancer agent, 4-amino tetrahydrocurcumin. *European Journal of Pharmaceutics and Biopharmaceutics*, 88(2), 351–360.
- Poonia, N., Kharb, R., Lather, V., & Pandita, D. (2016). Nanostructured lipid carriers: versatile oral delivery vehicle. *Future Science OA*, 2(3), FSO135.
- Prabaharan M. (2008). Chitosan derivatives as promising materials for controlled drug delivery. *Journal of Biomaterials Applications*, 23 (1), 5-36.
- Prabhu, R. H., Patravale, V. B., & Joshi, M. D. (2015). Polymeric nanoparticles for targeted treatment in oncology: current insights. *International Journal of Nanomedicine*, 10, 1001–1018.
- Puglia, C., & Bonina, F. (2012). Lipid nanoparticles as novel delivery systems for cosmetics and dermal pharmaceuticals. *Expert Opinion on Drug Delivery*, 9(4), 429–441.
- Purohit, K., Nandgude, D., & Poddar, S. (2016). Nano-lipid carriers for topical application: current scenario. *Asian Journal of Pharmaceutics*, 9(5), 1–9.

- Qi, L., Xu, Z., Jiang, X., Li, Y., & Wang, M. (2005). Cytotoxic activities of chitosan nanoparticles and copper-loaded nanoparticles. *Bioorganic & Medicinal Chemistry Letters*, 15(5), 1397–1399.
- Rabasco, M., & Rodríguez, M. (2000). Lipids in pharmaceutical and cosmetic preparations. *Grasas y Aceites*, 51, 74-96.
- Rapalli, V. K., Singhvi, G., Dubey, S. K., Gupta, G., Chellappan, D. K., & Dua, K. (2018). Emerging landscape in psoriasis management: From topical application to targeting biomolecules. *Biomedicine & Pharmacotherapy*, 106, 707–713.
- Rehman, M., Madni, A., Ihsan, A., Khan, W. S., Khan, M. I., Mahmood, M. A., . . . Shakir, I. (2015). Solid and liquid lipid-based binary solid lipid nanoparticles of diacerein: in vitro evaluation of sustained release, simultaneous loading of gold nanoparticles, and potential thermoresponsive behavior. *International Journal of Nanomedicine*, 10, 2805-2814.
- Rojek, B., & Wesolowski, M. (2019). DSC supported by factor analysis as a reliable tool for compatibility study in pharmaceutical mixtures. *Journal of Thermal Analysis and Calorimetry*, 138(6), 4531-4539.
- Rungphanichkul, N., Nimmannit, U., Muangsiri, W., & Rojsitthisak, P. (2011). Preparation of curcuminoid niosomes for enhancement of skin permeation. *Die Pharmazie*, 66(8), 570–575.
- Sandri, G., Bonferoni, M. C., Gökçe, E. H., Ferrari, F., Rossi, S., Patrini, M., & Caramella, C. (2010). Chitosan-associated SLN: in vitro and ex vivo characterization of cyclosporine A loaded ophthalmic systems. *Journal of Microencapsulation*, 27(8), 735–746.
- Sankalia, M. G., Mashru, R. C., Sankalia, J. M., & Sutariya, V. B. (2006). Reversed chitosan-alginate polyelectrolyte complex for stability improvement of alpha-amylase: optimization and physicochemical characterization. *European Journal of Pharmaceutics and Biopharmaceutics*, 65(2), 215-232.



- Sarmiento, B., Mazzaglia, D., Bonferoni, M., Cristina, N., Ana, M., & Maria, S. (2011). Effect of chitosan coating in overcoming the phagocytosis of insulin loaded solid lipid nanoparticles by mononuclear phagocyte system, *Carbohydrate Polymers*, 84(3), 919-925.
- Schäfer-Korting, M. (2010). Drug delivery. Springer Science & Business Media. 197.
- Segall, I. (2019). Preformulation: The use of FTIR incompatibility studies. *Journal of Innovations in Applied Pharmaceutical Science*, 4, 1-6.
- Sethacheewakul, S., Kedjinda, W., Maneenuan, D., & Wiwattanapatapee, R. (2011). Controlled release of oral tetrahydrocurcumin from a novel self-emulsifying floating drug delivery system (SEFDDS). *American Association of Pharmaceutical Scientists*, 12(1), 152–164.
- Shah, R. M., Malherbe, F., Eldridge, D., Palombo, E. A., & Harding, I. H. (2014). Physicochemical characterization of solid lipid nanoparticles (SLNs) prepared by a novel microemulsion technique. *Journal of Colloid and Interface Science*, 428, 286-294.
- Sharma, V., Anandhakumar, S., & Sasidharan, M. (2015). Self-degrading niosomes for encapsulation of hydrophilic and hydrophobic drugs: An efficient carrier for cancer multi-drug delivery. *Materials Science & Engineering. C, Materials for Biological Applications*, 56, 393–400.
- Sharma, V., Anandhakumar, S., & Sasidharan, M. (2015). Self-degrading niosomes for encapsulation of hydrophilic and hydrophobic drugs: An efficient carrier for cancer multi-drug delivery. *Materials Science & Engineering. C, Materials for Biological Applications*, 56, 393–400.
- Shi, F., Yang, G., Ren J., Guo, T., Du, Y., & Feng, N. (2013). Formulation design, preparation, and in vitro and in vivo characterizations of  $\beta$ -elemene-loaded nanostructured lipid carriers. *International Journal of Nanomedicine*, 8, 2533–2541
- Shrestha, H., Bala, R., & Arora, S. (2014). Lipid-based drug delivery systems. *Journal of Pharmaceutics*, 2014, 801820.

- Shukla, R.K., & Tiwari, A. (2012). Carbohydrate polymers: Applications and recent advances in delivering drugs to the colon. *Carbohydrate Polymers*, 88(2), 399-416.
- Silva, A. C., González-Mira, E., García, M. L., Egea, M. A., Fonseca, J., Silva, R., Santos, D., Souto, E. B., & Ferreira, D. (2011). Preparation, characterization and biocompatibility studies on risperidone-loaded solid lipid nanoparticles (SLN): high pressure homogenization versus ultrasound. *Colloids and Surfaces. B, Biointerfaces*, 86(1), 158–165.
- Silva, L. A., Andrade, L. M., de Sa, F. A., Marreto, R. N., Lima, E. M., Gratieri, T., & Taveira, S. F. (2016). Clobetasol-loaded nanostructured lipid carriers for epidermal targeting. *Journal of Pharmacy and Pharmacology*, 68(6), 742-750.
- Soleimanian, Y., Goli, S. A. H., Varshosaz, J., & Maestrelli, F. (2018). Propolis wax nanostructured lipid carrier for delivery of beta-sitosterol: Effect of formulation variables on physicochemical properties. *Food Chemistry*, 260, 97-105.
- Soma, D., Attari, Z., Reddy, S., Damodaram, A., & Koteswara, G. (2017). Solid lipid nanoparticles of irbesartan: preparation, characterization, optimization and pharmacokinetic studies. *Brazilian Journal of Pharmaceutical Sciences*, 53(1), 1-10
- Song, H., Moon, E. W., & Ha, J. H. (2021). Application of response surface methodology based on a Box-Behnken Design to determine optimal parameters to produce brined cabbage used in kimchi. *Foods (Basel, Switzerland)*, 10(8), 1935-1948.
- Song, S. H., Lee, K. M., Kang, J. B., Lee, S. G., Kang, M. J., & Choi, Y. W. (2014). Improved skin delivery of voriconazole with a nanostructured lipid carrier-based hydrogel formulation. *Chemical & Pharmaceutical Bulletin*, 62(8), 793–798.
- Sorasitthiyankarn, F. N., Muangnoi, C., Ratnatilaka Na Bhuket, P., Rojsitthisak, P., & Rojsitthisak, P. (2018). Chitosan/alginate nanoparticles as a promising

- approach for oral delivery of curcumin diglutaric acid for cancer treatment. *Materials Science & Engineering. C, Materials for Biological Applications*, 93, 178–190.
- Sun, R., Zhao, G., Ni, S., & Xia, Q. (2014). Lipid based nanocarriers with different lipid compositions for topical delivery of resveratrol: comparative analysis of characteristics and performance. *Journal of Drug Delivery Science and Technology*, 24(6), 591-600.
- Sütő, B., Berkó, S., Kozma, G., Kukovecz, Á., Budai-Szűcs, M., Erős, G., Kemény, L., Sztojkov-Ivanov, A., Gáspár, R., & Csányi, E. (2016). Development of ibuprofen-loaded nanostructured lipid carrier-based gels: characterization and investigation of in vitro and in vivo penetration through the skin. *International Journal of Nanomedicine*, 11, 1201–1212.
- Sutradhar KB., & Amin M. (2014). Nanotechnology in cancer drug delivery and selective targeting. *International Scholarly Research Notices*. 2014, 1-12
- Tanwar H., & Sachdeva R. (2016). Transdermal drug delivery system: a review. *International Journal of Pharmaceutical Sciences and Research*, 7, 2274-2290.
- Tavares, M., Santos Rosa Viegas, J., Palma Abriata, J., Viegas, F., Testa Moura de Carvalho Vicentini, F., Lopes Badra Bentley, M. V., Tapia-Blacido, D. R. (2021). Design of experiments (DoE) to develop and to optimize nanoparticles as drug delivery systems. *European Journal of Pharmaceutics and Biopharmaceutics*, 165, 127-148.
- Taveira, S. F., De Santana, D. C., Araujo, L. M., Marquele-Oliveira, F., Nomizo, A., & Lopez, R. F. (2014). Effect of iontophoresis on topical delivery of doxorubicin-loaded solid lipid nanoparticles. *Journal of Biomedical Nanotechnology*, 10(7), 1382-1390.
- Tobin, A. M., & Kirby, B. (2005). TNF alpha inhibitors in the treatment of psoriasis and psoriatic arthritis. *BioDrugs: Clinical Immunotherapeutics, Biopharmaceutics and Gene Therapy*, 19(1), 47–57.

- Tonel, G., & Conrad, C. (2009). Interplay between keratinocytes and immune cells-- recent insights into psoriasis pathogenesis. *The International Journal of Biochemistry & Cell Biology*, 41(5), 963–968.
- Torsekar, R., & Gautam, M. M. (2017). Topical Therapies in Psoriasis. *Indian Dermatology Online Journal*, 8(4), 235–245.
- Tran, T. H., Ramasamy, T., Truong, D. H., Choi, H. G., Yong, C. S., & Kim, J. O. (2014). Preparation and characterization of fenofibrate-loaded nanostructured lipid carriers for oral bioavailability enhancement. *AAPS PharmSciTech*, 15(6), 1509–1515.
- Trivedi, M. K., Panda, P., Sethi, K. K., Gangwar, M., Mondal, S. C., & Jana, S. (2020). Solid and liquid state characterization of tetrahydrocurcumin using XRPD, FT-IR, DSC, TGA, LC-MS, GC-MS, and NMR and its biological activities. *Journal of Pharmaceutical Analysis*, 10(4), 334-345.
- Uner, M. (2006). Preparation, characterization and physico-chemical properties of solid lipid nanoparticles (SLN) and nanostructured lipid carriers (NLC): their benefits as colloidal drug carrier systems. *Die Pharmazie*, 61(5), 375–386.
- Uner, M., & Yener, G. (2007). Importance of solid lipid nanoparticles (SLN) in various administration routes and future perspectives. *International Journal of Nanomedicine*, 2(3), 289–300.
- Vecchione, R., Ciotola, U., Sagliano, A., Bianchini, P., Diaspro, A., & Netti, P. A. (2014). Tunable stability of monodisperse secondary O/W nano-emulsions. *Nanoscale*, 6(15), 9300-9307.
- Velmurugan, R., & Selvamuthukumar, S. (2015). Development and optimization of ifosfamide nanostructured lipid carriers for oral delivery using response surface methodology. *Applied Nanoscience*, 6(2), 159-173.
- Venancio, J. H., Andrade, L. M., Esteves, N. L. S., Brito, L. B., Valadares, M. C., Oliveira, G. A. R., & Taveira, S. F. (2017). Topotecan-loaded lipid nanoparticles as a viable tool for the topical treatment of skin cancers. *Journal of Pharmacy and Pharmacology*, 69(10), 1318-1326.

- Verma, R. K., & Garg, S. (2005). Selection of excipients for extended release formulations of glipizide through drug-excipient compatibility testing. *Journal of Pharmaceutical and Biomedical Analysis*, 38(4), 633-644
- Wang, F., Chen, J., Dai, W., He, Z., Zhai, D., & Chen, W. (2017). Pharmacokinetic studies and anticancer activity of curcumin-loaded nanostructured lipid carriers. *Acta Pharmaceutica (Zagreb, Croatia)*, 67(3), 357-371.
- Wcisło-Dziadecka, D., Zbiciak-Nylec, M., Brzezińska-Wcisło, L., & Mazurek, U. (2016). TNF- $\alpha$  in a molecularly targeted therapy of psoriasis and psoriatic arthritis. *Postgraduate Medical Journal*, 92(1085), 172-178.
- Wissing, S. A., & Müller, R. H. (2003). Cosmetic applications for solid lipid nanoparticles (SLN). *International Journal of Pharmaceutics*, 254(1), 65-68.
- Wissing, S. A., Kayser, O., & Muller, R. H. (2004). Solid lipid nanoparticles for parenteral drug delivery. *Advanced Drug Delivery Reviews*, 56(9), 1257-1272.
- Witayaudom, P., & Klinkesorn, U. (2017). Effect of surfactant concentration and solidification temperature on the characteristics and stability of nanostructured lipid carrier (NLC) prepared from rambutan (*Nephelium lappaceum* L.) kernel fat. *Journal of Colloid and Interface Science*, 505, 1082-1092.
- Woo, Y. R., Cho, D. H., & Park, H. J. (2017). Molecular mechanisms and management of a cutaneous inflammatory disorder: psoriasis. *International journal of molecular sciences*, 18(12), 2684.
- Woraphatphadung, T., Sajomsang, W., Rojanarata, T., Ngawhirunpat, T., Tonglairoum, P., & Opanasopit, P. (2018). Development of chitosan-based pH-sensitive polymeric micelles containing curcumin for colon-targeted drug delivery. *AAPS PharmSciTech*, 19(3), 991-1000.
- Xiao, B., Chen, Q., Zhang, Z., Wang, L., Kang, Y., Denning, T., & Merlin, D. (2018). TNF $\alpha$  gene silencing mediated by orally targeted nanoparticles combined with interleukin-22 for synergistic combination therapy of ulcerative colitis. *Journal of Controlled Release*, 287, 235-246.

- Yan, Q., Chen, X., Gong, H., Qiu, P., Xiao, X., Dang, S., Hong, A., & Ma, Y. (2018). Delivery of a TNF- $\alpha$ -derived peptide by nanoparticles enhances its antitumor activity by inducing cell-cycle arrest and caspase-dependent apoptosis. *The FASEB Journal*, 32 (12), 6948-6964.
- Yin, L., & Zhong, Z. (2020). *Nanoparticles*. Biomaterials Science. Elsevier, Oxford, 453-484.
- Yousef, S., Mohammed, Y., Namjoshi, S., Grice, J., Sakran, W., & Roberts, M. (2017). Mechanistic evaluation of hydration effects on the human epidermal permeation of salicylate esters. *The AAPS Journal*, 19(1), 180–190.
- Yu, Y., Feng, R., Yu, S., Li, J., Wang, Y., Song, Y., Yang, X., Pan, W., & Li, S. (2018). Nanostructured lipid carrier-based pH and temperature dual-responsive hydrogel composed of carboxymethyl chitosan and poloxamer for drug delivery. *International Journal of Biological Macromolecules*, 114, 462–469.
- Yuan, Y., Chesnutt, M., Haggard, O., & Bumgardner, D. (2011). Deacetylation of chitosan: material characterization and in vitro evaluation via albumin adsorption and pre-osteoblastic cell cultures. *Materials*, 4(8), 1399-1416.
- Yuyun, Y., Ratnatilaka Na Bhuket, P., Supasena, W., Suwattananuruk, P., Praengam, K., Vajragupta, O., Muangnoi, C., & Rojsitthisak, P. (2021). A novel curcumin-mycophenolic acid conjugate inhibited hyperproliferation of tumor necrosis factor-alpha-induced human keratinocyte cells. *Pharmaceutics*, 13(7), 956.
- Zhang, T., Chen, J., Zhang, Y., Shen, Q., & Pan, W. (2011). Characterization and evaluation of nanostructured lipid carrier as a vehicle for oral delivery of etoposide. *European Journal of Pharmaceutical Sciences*, 43(3), 174–179.
- Zhang, Y., Huo, M., Zhou, J., Zou, A., Li, W., Yao, C., & Xie, S. (2010). DDSolver: an add-in program for modeling and comparison of drug dissolution profiles. *American Association of Pharmaceutical Scientists Journal*, 12(3), 263-271.

Zhao, X., Chen, Q., Li, Y., Tang, H., Liu, W., & Yang, X. (2015). Doxorubicin and curcumin co-delivery by lipid nanoparticles for enhanced treatment of diethylnitrosamine-induced hepatocellular carcinoma in mice. *European Journal of Pharmaceutics and Biopharmaceutics*, 93, 27–36.

Zhao, X., Chen, Q., Li, Y., Tang, H., Liu, W., & Yang, X. (2015). Doxorubicin and curcumin co-delivery by lipid nanoparticles for enhanced treatment of diethylnitrosamine-induced hepatocellular carcinoma in mice. *European Journal of Pharmaceutics and Biopharmaceutics*, 93, 27–36.



## VITA

<b>NAME</b>	Truong Hoang Thien
<b>DATE OF BIRTH</b>	25 April 1996
<b>PLACE OF BIRTH</b>	Vietnam
<b>INSTITUTIONS ATTENDED</b>	Faculty of Pharmaceutical Sciences

